Review

Fluid–Structure Interaction Aortic Valve Surgery Simulation: A Review

Alex G. Kuchumov [1,2,*] , Anastasiya Makashova [1], Sergey Vladimirov [3], Vsevolod Borodin [3] and Anna Dokuchaeva [3]

1 Department of Computational Mathematics, Mechanics and Biomechanics, Perm National Research Polytechnic University, 614990 Perm, Russia; derrysns@gmail.com
2 Biofluids Laboratory, Perm National Research Polytechnic University, 614990 Perm, Russia
3 Meshalkin National Medical Research Center, 630055 Novosibirsk, Russia; sergvlad89@gmail.com (S.V.); b.vsevolod97@yandex.ru (V.B.); a_dokuchaeva@meshalkin.ru (A.D.)
* Correspondence: kychymov@inbox.ru

Abstract: The complicated interaction between a fluid flow and a deformable structure is referred to as fluid–structure interaction (FSI). FSI plays a crucial role in the functioning of the aortic valve. Blood exerts stresses on the leaflets as it passes through the opening or shutting valve, causing them to distort and vibrate. The pressure, velocity, and turbulence of the fluid flow have an impact on these deformations and vibrations. Designing artificial valves, diagnosing and predicting valve failure, and improving surgical and interventional treatments all require the understanding and modeling of FSI in aortic valve dynamics. The most popular techniques for simulating and analyzing FSI in aortic valves are computational fluid dynamics (CFD) and finite element analysis (FEA). By studying the relationship between fluid flow and valve deformations, researchers and doctors can gain knowledge about the functioning of valves and possible pathological diseases. Overall, FSI is a complicated phenomenon that has a great impact on how well the aortic valve works. Aortic valve diseases and disorders can be better identified, treated, and managed by comprehending and mimicking this relationship. This article provides a literature review that compiles valve reconstruction methods from 1952 to the present, as well as FSI modeling techniques that can help advance valve reconstruction. The Scopus, PubMed, and ScienceDirect databases were used in the literature search and were structured into several categories. By utilizing FSI modeling, surgeons, researchers, and engineers can predict the behavior of the aortic valve before, during, and after surgery. This predictive capability can contribute to improved surgical planning, as it provides valuable insights into hemodynamic parameters such as blood flow patterns, pressure distributions, and stress analysis. Additionally, FSI modeling can aid in the evaluation of different treatment options and surgical techniques, allowing for the assessment of potential complications and the optimization of surgical outcomes. It can also provide valuable information on the long-term durability and functionality of prosthetic valves. In summary, fluid–structure interaction modeling is an effective tool for predicting the outcomes of aortic valve surgery. It can provide valuable insights into hemodynamic parameters and aid in surgical planning, treatment evaluation, and the optimization of surgical outcomes.

Keywords: aortic valve; aortic valve model; computational fluid dynamics; biological and mechanical aortic valves; transcatheter aortic valve replacement; fluid–solid interaction method

1. Introduction

Millions of patients suffer from aortic valve diseases, which reveals a global problem [1–3]. Currently, in the United States, the overall prevalence of mitral or aortic valvular heart disease in the context of a patient's age is estimated at 2.5% of the general population, and in people older than 75 years, it exceeds 10%. Assuming the aging population worldwide, the prevalence of such pathologies is expected to grow exponentially [4,5]. In Russia, diseases of the circulatory

system account for 47% of the causes of mortality [6]. According to the European Society of Cardiology, Russia belongs to countries with a very high risk of CVD, as cardiovascular mortality exceeds 450 cases per 100,000 population for men and over 350 cases for women [7]; also, mortality from CVD increased by 12% according to 2021 research data [8]. One of the ways of helping to manage valve disease is the use of mathematical modeling and biomechanical methods, using computer tools to support medical diagnosis and design of prostheses, as well as providing many predictive data that contemporary imaging methods cannot provide [9–16]. CFD and FSI approaches have gained a wide spread within several last decades [17–20]. This review is conditionally divided into two parts (Figure 1); the first one is devoted to the aortic valves, pathologies, and methods of reconstruction for different types of valve prostheses. The second part consists of an overview of mathematical modeling that may help the outcome of valve replacement (Table 1), including models of transcatheter valve replacement, comparison valves made of bovine and porcine pericardium, numerical modeling at various scales (tissue and cellular), and predictions of the Ozaki procedure. The aim of this work is to demonstrate the progress of computer modeling methodology, as well as to systematize knowledge about the treatment of heart valve disease from the 20th century to the present day so the researchers can analyze the approaches used by their predecessors.
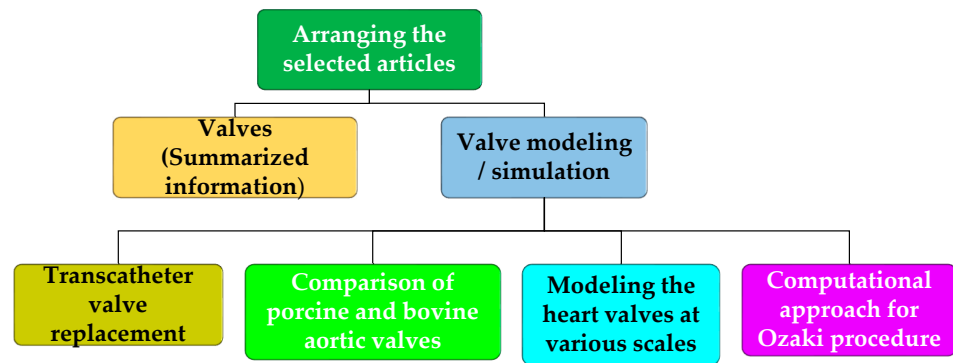

Figure 1. Flowchart of the review.

Table 1. Some examples of aortic valve numerical modeling.

Article + Year	Application	Revised Model	Personalized Model	Analyzed Characteristics
Michael et al. 2019 [21]	TAVR	FSI	No	Radial force
Bosi et al. 2018 [22]	TAVR	Matlab, Abaqus	Yes	Influence of chosen material on valve diameter
Amindari et al. 2021 [23]	TAVR	FSI	No	Aortic ring size, valve area, jet velocity
Mao et al. 2018 [24]	TAVR	CFD	Yes	Deployment height
Sturla et al. 2013 [25]	Aortic root	FSI	No	Tissue deformation and stress
Wu et al. 2016 [26]	TAVR	FSI	Yes	Pressure and velocities
Kalyana et al. 2015 [27]	Aortic valve	FSI	No	Pressure and flow
Tzamtzis et al. 2013 [28]	TAVR	MSC	No	Radial force

Table 1. *Cont.*

Article + Year	Application	Revised Model	Personalized Model	Analyzed Characteristics
Bosmans et al. 2016 [29]	TAVR	FEM	Yes	Influence of chosen material on valve diameter, leakage
Finotello et al. 2017 [30]	TAVI	Matlab, Abaqus	Yes	Material properties, discretization
Wang et al. 2015 [31]	TAVI	FSI	No	Stress
Dowling et al. 2019 [32]	TAVR	CFD	Yes	Size and depth of implantation
Bianchi et al. 2019 [33]	TAVR	CFD	Yes	Depth of implantation, stress, pressure, velocities, contact force, contact surface
Whelan et al. 2018 [34]	Bovine valve	Uniaxial tension	No	Tensile strength, strength at break, fatigue performance
Travaglino et al. 2020 [35]	Transcatheter aortic valve	Bayesian optimization	No	Stress, contact surface
Loon et al. 2004 [36]	Aortic valve	FSI	No	Pressure, shear stress, velocity
Li et al. 2021 [37]	Porcine and bovine valves	FSI	No	Blood flow velocity, systolic transverse pressure gradient, geometric surface, flux shear stress, strain/stress
Weinberg et al. 2008 [38]	Bicuspid and tricuspid valves	FSI	No	Deformation, dynamic tension, dependence of fluid velocity on radial position, surface curvature, dynamic proportions of cells
Hart et al. 2003 [39]	Aortic valve	FSI	No	Flow velocity, pressure
Nicosia et al. 2003 [40]	Aortic valve, aortic root	FEM LS-Dyna	No	Flow velocity, material
Weinberg et al. 2005 [41]	Valve cusps	FEM	No	Tissue deformation
Stella et al. 2007 [42]	Valve cusps	Biaxial tension	No	Radial stress, thickness
Weinberg et al. 2006 [43]	Valve cusps	FEM	No	Wall shear stress, strain
Liu et al. 2022 [44]	TAVI	FSI	No	Flow velocity, maximum principal stress distribution
Pil et al. 2023 [45]	Valve cusps	FSI	No	Wall shear stress, OSI, TAWSS
Abdi et al. 2023 [46]	Aortic root, aortic valve	FSI	No	Wall shear stress, OSI, TAWSS
Bosi et al. 2020 [47]	TAVI	FSI	Yes	max principal strain, prosthesis deployment
Morany et al. 2023 [48]	Aortic valve, aortic root	FSI	No	Velocity, maximum principal stress distribution, wall shear stress

2. Materials and Methods

A systematic literature search was carried out before 30 April 2023 using keywords such as aortic valve, FSI modeling, TAVR, Ozaki procedure, bioprosthetic valves, mechanical valve, and others.

A search scheme for Scopus, Pubmed, and ScienceDirect databases is presented below (Figure 2). A total of 162 articles were included.
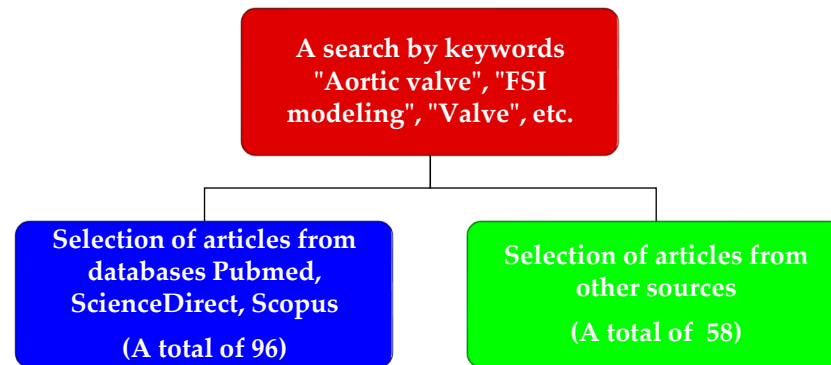

Figure 2. Flowchart of the research.

The procedure for selecting studies went as follows: Initially, relevant articles were selected from the databases and organized in an Excel spreadsheet. Repeated entries were then removed. The inclusion criteria for articles were restricted to (1) a survey of the methodological literature on aortic valves since aortic insufficiency, along with mitral heart valve pathologies, is among the most frequent diseases in cardiology. Other criteria used to exclude studies were (2) notes from conference proceedings, (3) abstract comments, (4) studies with geometries from animals other than porcine and bovine, and (5) computational methods on polymer valves as their clinical testing in humans is currently very limited.

2.1. Aortic Valves

A normally formed tricuspid aortic valve (AV) consists of three semilunar leaflets [49]. The aortic valve is located between the left ventricular outflow tract and the ascending aorta. The fibrous ring (annulus fibrosus, AF) of the AV has a cylinder shape in which the valve is fixed in the form of a crown [50,51]. The aortic root is a valvular–aortic complex consisting of the annulus fibrosus (AF) of the AV, semilunar cusps, sinuses of Valsalva, commissural rods, and arches connecting the tops of the commissures. Forming the outflow tract of the left ventricle, the function of the aortic root structure is to maintain the elements of the aortic valve [52].

The AV has two states: open in systole, when blood flows from the ventricle into the aorta, and closed in diastole when the direction of blood flow is reversed, but the reverse flow is prevented by the leaflets' closing (Figure 3) [53,54]. At this stage, two specific valve pathologies can be distinguished—aortic stenosis and aortic insufficiency (Figure 4).

Aortic insufficiency (AI) is the absence of complete closure of the aortic valve cusps in diastole and the occurrence of reverse blood flow (regurgitation) from the aorta to the cavity of the left ventricle [55]. In case of severe insufficiency, up to 60% of the systolic blood volume can return to the left ventricle [56].
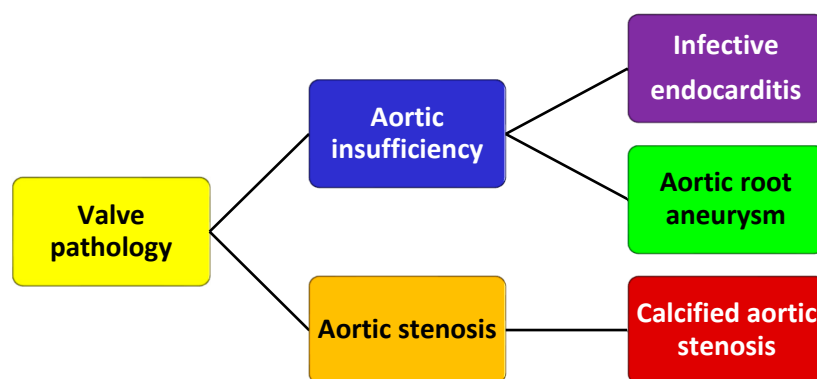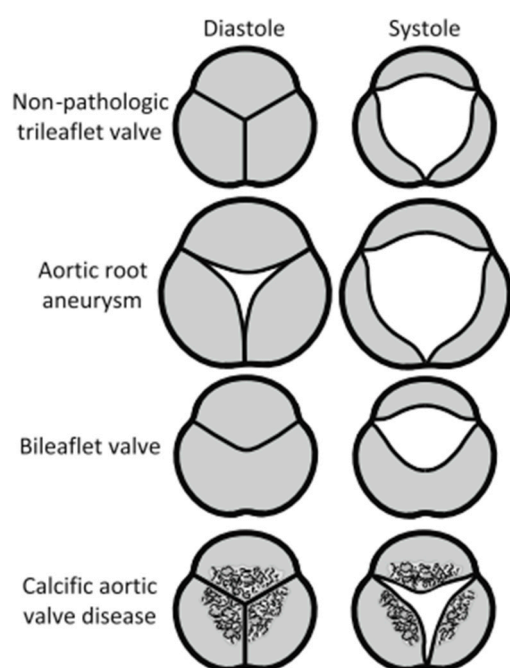
Figure 3. Valve pathology flowchart.

Figure 4. Geometry of the valve behavior for different pathologies in systole and diastole.

AI can be caused by a congenital malformation of the aortic valve leaflets and/or abnormalities in the geometry of the aortic root and ascending aorta. Some of the reasons lead to the slow development of chronic aortic regurgitation and induce physiological compensation, while others lead to the sudden onset of acute aortic regurgitation. Most often, with the development of chronic AI, slow compensatory LV dilatation, and eccentric myocardium hypertrophy are observed, which maintains the sufficiency of cardiac output.

The causes of AI may be (Figure 3) aortic root aneurysm, infective endocarditis, congenital aortic deformities, calcific degenerations, rheumatic diseases, systemic hypertension, myxomatous degeneration, and ascending aortic dissection, as well as Marfan syndrome [57].

If aortic regurgitation develops rapidly, physiological compensation does not occur promptly, which entails acute and severe regurgitation, a sudden catastrophic increase in LV diastolic pressure, and a decrease in cardiac output. The development of acute AI can be a result of infective endocarditis, chest trauma, and aortic dissection [58].

The main causes of AV insufficiency are infective endocarditis and aortic root aneurysm [59]. Aortic root aneurysms are prone to aortic dissection [60,61], with dilatation of the thoracic aorta occurring in about 40% of patients [62]. It is also common for patients with this disease to have

a bicuspid aortic valve (BAV), which is the most common congenital heart disease and occurs in 1–2% of the population [63]. The geometries of the bicuspid valve are shown in Figure 5.
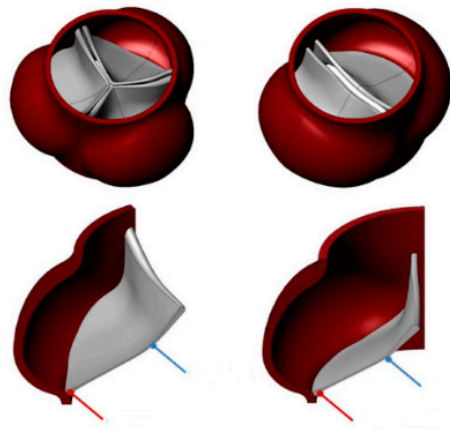

Figure 5. Valve geometry types. Left: tricuspid. Right: bicuspid. Top: complete valve geometry. Bottom: cutouts showing tracking locations.

There are controversies about the heritability of BAV, but more and more evidence points to the genetic cause of its occurrence [64–68]. The fact that the presence of BAV predisposes to a number of tissue diseases, including aortic dilatation and dissection, also suggests that the defect is accompanied by dysfunction of the tissue structure [43,66,69–72].

Aortic stenosis is a narrowing of the left ventricular outflow tract in the region of the aortic valve, leading to difficulty in the blood outflow from the left ventricle to the aorta and a sharp increase in the pressure gradient between them [73].

Aortic stenosis can be caused by rheumatic disease or, more commonly, by calcification of a native bicuspid or tricuspid valve (Figure 3) [74]. There is a correlation between the prevalence of aortic stenosis and the increasing age of patients. The distribution of AS increases from 0.2% in the group aged 50–59 years to 9.8% in the group of patients 80–89 years old. It is assumed that the prevalence of AS in the population is increasing due to increasing life expectancy and the aging of the population. It should be clarified that AS is the most common reason for aortic valve replacement [75].

Calcified aortic valve stenosis (CAS) is caused by the accumulation of calcium in the tissues and mineral conglomerate thickening, which leads to poor blood flow from the left ventricle to the aorta. In Western countries, CAS has become the third most common cardiovascular disease in elderly patients, after coronary heart disease and hypertension [76].

In developed countries, aortic stenosis caused by rheumatic disease is rare and generally occurs in conjunction with mitral valve disease. In this case, adhesive fusion of the valve is characteristic, in contrast to calcified AC [77,78].

The classic surgical technique for CAS is the replacement of the affected valve with a prosthesis [79,80]. Currently, three main types of artificial heart valves (Figure 6) are mechanical, bioprosthetic, and tissue-engineered valves [81]. A perfect heart valve prosthesis should precisely replicate the characteristics of a normal heart valve and hemodynamics, but currently available valve prostheses do not meet these requirements. Thus, patients undergoing transcatheter implantation of a heart valve bioprosthesis are at an increased risk of thromboembolism in the first few months [82–84]. None of the currently available heart valve prostheses have the ability to fully grow, repair, remodel, and regenerate.
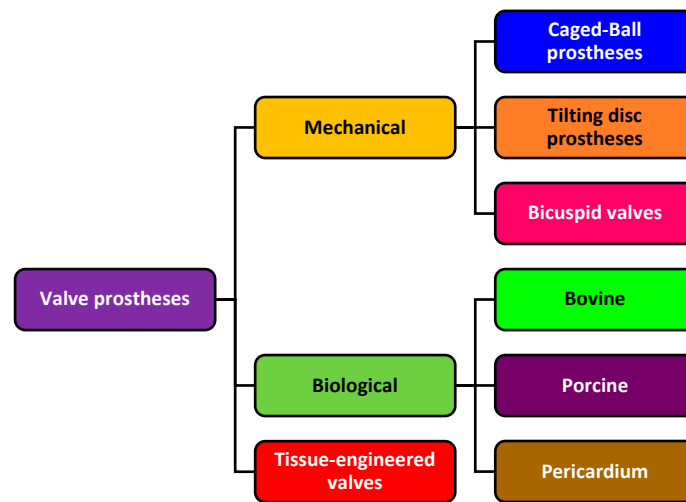
Figure 6. Flowchart of prosthetic valve types.

2.2. Mechanical Valve Prostheses

The first mechanical prosthetic aortic valve was successfully implanted in 1952, and in 1960, a replacement of the mitral valve was performed [84–86]. The first bicuspid valve was introduced by St. Jude Medical Inc., which has undergone many changes over the past decades [87].

There are several types of mechanical valves (Figure 7) such as ball valves, which were mainly used from 1965 to 1967 in which most of the complications with them were associated with severe pressure changes caused by obstruction of the blood flow [88]; and tilt-plate valves, which were created to overcome the hemodynamic problems of ball valves and bicuspid valves.

Figure 7. Types of mechanical valves.

The main advantage of mechanical valves is their durability; nevertheless, their use is associated with a significant risk of thrombogenicity and the need for lifelong anticoagulation therapy to prevent blood clotting. The complications associated with these valves make them undesirable for some patients, such as pregnant women and injured people [89,90]. However, mechanical valves may be safer for some patients, especially younger ones [91].

2.3. Biological Valve Prostheses

About 40–60% of the world's heart valve replacement operations are carried out with the use of biological prostheses produced using animal tissues (bovine (Figure 8) or porcine) fixed in glutaraldehyde (GA) [92–95]. GA treatment prevents the denaturation of the collagen structure; however, such treatment is known to accelerate the calcification of the prosthesis [96]. Bioprosthetic heart valves (BHVs) are less thrombogenic than mechanical ones, have more natural hemodynamic characteristics, lower pressure gradients, and a

larger orifice area [97,98]. The main disadvantages of BHVs include almost 4 times lower durability and up to 15% chances of thromboembolic complications, possibly associated with a rougher fibrous surface of the biological tissue of the prosthesis [99].

Figure 8. Bovine biological heart valve prosthesis.

The main advantage of BHVs is the possibility of their implantation using a minimally invasive technique called transcatheter aortic valve implantation (TAVI), which is currently approved for patients with any level of surgical risk [3,100]. Since 2002, when the TAVI procedure was first introduced, a variety of prostheses, different in their design parameters, have been developed; the biological materials of the leaflets, methods of their processing, shapes and materials of prosthesis frameworks, etc. were changed [101,102]. Transcatheter implantation is a novel alternative method for correcting aortic stenosis in patients considered inoperable or at high risk of traditional aortic valve replacement [103–105]. But currently, unpleasant consequences such as problems with flap durability, paraclap leaks, and the occurrence of thrombosis persist [106].

Over time, the functioning of BHVs containing biological tissue treated with GA begins to deteriorate, which occurs over 1–2 decades and is explained by the immune response and calcification [107]. Long-term studies have shown that the incidence of structural valve degeneration 15 years after implantation is between 30% and 60%, which is partly caused by the process of calcium accumulation [108] associated with the level of mechanical stress [109].

2.4. Advanced Developments in the Field of Heart Valves

An advanced approach to aortic valve reconstruction with favorable initial results was developed called the Ozaki procedure [110–112]. The authors stated that their procedure can be applied to a wide range of aortic valve diseases, including aortic stenosis, aortic regurgitation, and others. The Ozaki procedure consists of the replacement of three native aortic leaflets with leaflets made from the patient's own pericardium. One of the advantages of this technique is the preservation of aortic root hemodynamics while providing a more efficient valve orifice area [113].

A xenogeneic valve was obtained from biological tissue. To avoid its rejection, cellular antigen and nucleic acid residues are removed (i.e., to decellularize biomaterials—to remove cells and nucleic acids in the extracellular matrix to reduce the immunogenicity of biomaterials from non-autologous sources). Several studies have shown that the combined decellularization method can not only increase the decellularization efficiency but also maximize the protection of the extracellular matrix [114,115], which prevents calcification.

Valves made of flexible polymeric materials such as polytetrafluorethylene (PTFE), poly(styrene-block-isobutylene-block-styrene) (SIBS), and polyurethane (PU) have also emerged as potential candidates for heart valve prostheses [116,117]. First, they can be mass-produced compared to the limited sources and high cost of biological valves, and

second, they have precisely regulated physical and biochemical properties. However, the greatest challenges for them remain prosthesis failure due to the difference in elastic modulus between polymers and native tissue and durability [115,118,119].

3. Numerical Simulation

3.1. Valve Modeling

Numerical approaches are currently widely used in clinical practice to study biofluid-flow parameters and their changes under pathological conditions [12,19,20,120,121]. There are three main classes of relevant computational models (Figure 9): FE, CFD, and Fluid–Structure Interaction (FSI) analysis. FE models cover only the structural region, such as the aortic root and native and prosthetic valve leaflets. This type of analysis allows one to study structures by solving mechanical continuum equations. CFD simulation provides information about the pressure and velocity fields in the fluid domain by solving the continuity and Navier–Stokes equations [122–124]. This approach does not take into account structural fields and therefore does not allow the assessment of structures such as valve motion. To perform an accurate dynamic analysis that includes modeling of blood flow during the cardiac cycle in combination with the structural mechanics of the valve, FSI analysis is necessary because it considers both the structural and fluid flow domains [125,126].
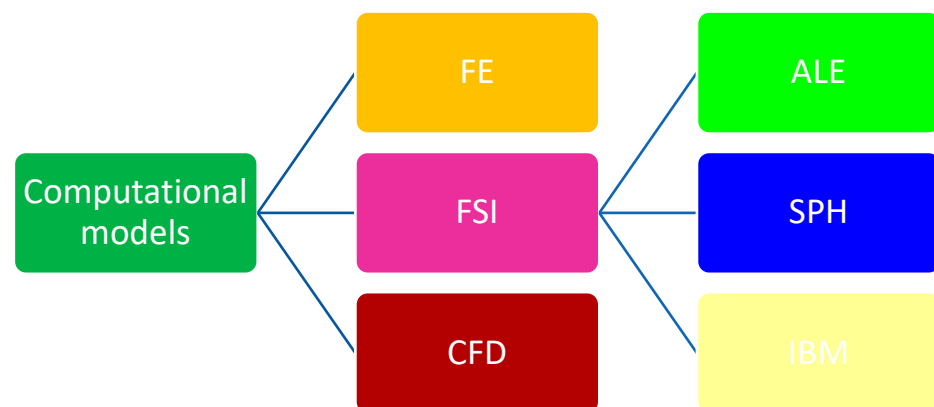

Figure 9. Flowchart of computational models.

The Arbitrary Lagrange–Euler method (ALE) [45], smoothed-particle hydrodynamics (SPH) [127], and the IBM (immersed boundary method), as well as the Lattice Boltzmann Method [48] are currently the three most popular methods for solving FSI problems in hemodynamic studies. The ALE and SPH methods are commonly used to study blood flow in the cardiovascular system and its interaction with rigid bodies, such as mechanical valves [128–133]. However, the instability of the adaptive remeshing algorithm, high cost, and tedious determination process limit their use for bioprosthesis valve modeling [134], which involves complex contact and FSI problems during transient computation [135–148]. Although it is now possible to reduce the computational costs somewhat by using the direct interaction scheme (IB-LBM), adding the immersed boundary method (IBM) as a boundary force calculator (it is a combination of the positive aspects of both methods, such as the use of a Cartesian grid and the ability to perform algebraic operations in parallel) [149–151]. However, parameters are constantly being added that should be paid attention to during modeling; previously, the mechanics of the leaflets were most often considered, but now it is also necessary to take into account the distribution of pressure on the surface of the leaflets, the balance of the momentum of the flow, the dynamics of eddies during aortic curvature, and the distribution of shear stress; the relationship between kinetic energy and spirality in prosthetic hemodynamic is poorly understood [152–158].

The use of coarse mesh [159], increased viscosity [155], or trimming the computational power to the pipeline-type models [160] is necessary due to large jet flows, strong boundary layer detachment, vortex and stall formation, and high nonlinear and instantaneous valve

deformation. All of these can threaten the physiological accuracy of the calculations and require appropriate compromises in the use of computational and time resources.

Also, the lack of medical data plays an important role. For example, studies that show potential significant improvements in transvalvular systolic gradient, blood flow, aortic valve orifice area, and cardiac output after TAVR are difficult to quantify due to the lack of data on structurally normal native heart valves, and it is also difficult to determine the optimal flow profile because it requires prediction of valve size, design type, and orientation [161,162]. However, the progress of research does not stand still, and improvements in numerical method models are constantly being applied.

3.2. Numerical Simulation of Transcatheter Valve Replacement

However, some complex problems are already being solved with the help of numerical methods. For example, the basis for modeling the TAVI operation was created [21], and a number of patient-specific models that reproduce the process of valve replacement were developed [22,163]. These models can be used as information support for surgeons when planning a surgical intervention before transcatheter valve implantation.

When calculating them, the following are determined: geometric (the size of the aortic ring), kinematic (the area of the aortic valve), and hydrodynamic (the velocity of the bloodstream) characteristics [164]. It was also found that the characteristics of the material strongly affect the deformation of the leaflets in the systolic phase [23]. Moreover, the anisotropic behavior of both stent and leaflet should be included when assessing the fatigue life of TAVR systems [165,166].

Liu et al. [44] proved that it is possible to reduce the load on the leaflets and stents of the model by changing the geometry of the petals, which increases the reliability of the stent design and reduces the possibility of thrombosis since most studies did not include the relationship between structural design and flow fields, and also did not conduct relevant parametric studies, since they used the characteristics of valves already available on the market [167,168] or the models were too simplified [169]. This is consistent with a study by Govidarajan et al. [170], which suggested that efficient valve opening could reduce energy loss.

As clinical data are often limited in information content, boundary conditions (BC) for dynamic modeling are often specified as idealized dependences of inlet and outlet pressures or flows and are applied to the left ventricular outflow tract and ascending aorta, respectively [171,172].

Some researchers [27] indicate that these methods have limitations that question the clinical relevance of studies conducted using them. Thus, when setting BC using a strict definition of flow, regurgitation in the diastolic phase is determined in advance, which does not allow adequate assessment of the physiological characteristics of the valve. Regurgitation is a function of valve characteristics and cannot be predetermined. On the other hand, when determining BC using a pressure gradient at the inlet and outlet of the valve, the physiological blood flow that is created by the left ventricle is not ensured, regardless of the pathology and valve resistance. Based on this, a variant of the combined method of setting the BC is described, namely in systole, which is proposed to set the blood flow provided by the left ventricle, and in diastole, which is proposed to set the pressure gradient on the valve caused by the residual blood pressure.

It should be clarified that numerical modeling is widely used for both self-expanding and balloon-expandable transcatheter heart valve prostheses [28–30,44]. Thus, retrospective modeling of a balloon-expandable valve based on stress fields revealed a high load in the aortic sinus (Figure 10). This analysis is promising for predicting adverse outcomes, such as aortic root rupture, conduction disturbance, and the presence of leakage between the implanted valve and surrounding tissue structure [24,31–33,173,174]. In particular, numerical modeling is a potential solution for the problem of predicting the outcome of the transcatheter replacement with BAVs, as this operation remains challenging because the

incidence of paravalvular regurgitation and the need for a permanent pacemaker is higher than with open surgery [175–177].
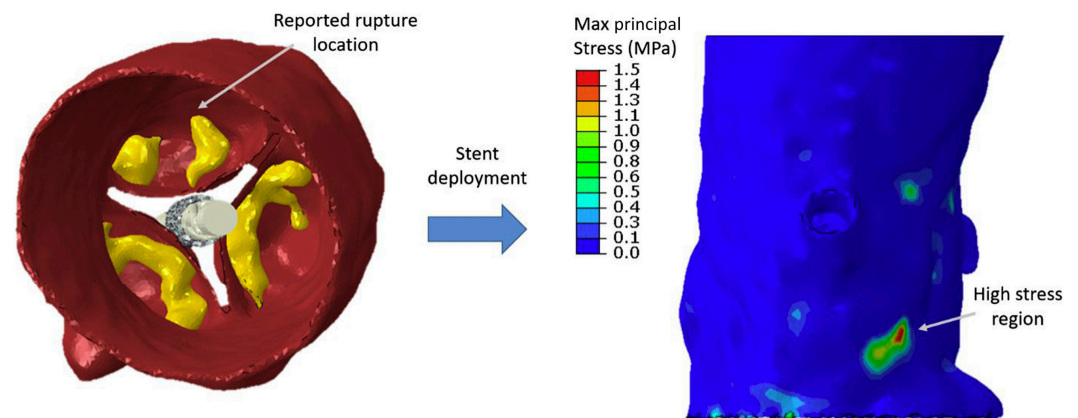

Figure 10. SAPIEN S3 transcatheter heart valve deployment in a patient who experienced aortic root rupture with detection of high stress in the region where the rupture occurred [178].

3.3. Numerical Modeling for Comparison of Porcine and Bovine Aortic Valves

FSI methods are not only used to model transcatheter valve implantation; for example, they allow the comparison of porcine and bovine aortic valves, which were clinically proven to be reliable in various characteristics [96,179,180]. The influence of the properties of both bovine and porcine pericardium on the design of a transcatheter aortic valve at a pressure of 120 mm Hg [35], and the effect of valve bore shape and stiffness on blood flow to assess valvular dysfunctions were studied [36]. It was also suggested that a bovine pericardial valve has better hemodynamic characteristics [181–183]. In addition, since the orientation of collagen fibers is a key factor influencing the strength and fatigue characteristics of pericardial tissue, some results suggest that unscreened (the process of optimum collagen fiber direction identification) porcine pericardial tissue will have more stable mechanical properties [96].

Li et al. [37] compared maximum flow rate, maximum pressure, pressure gradient, geometric orifice area, and shear flow stress; it was also shown that bovine pericardial valves have better hemodynamic characteristics and lower leaflet loading compared to porcine pericardial valves. The mean and peak net pressure gradients for the four bovine aortic valve models were 8.1% and 8.4% lower than for the porcine pericardium aortic valve models, respectively.

In addition, larger valves for both porcine and bovine aortic valves have shown better hemodynamic performance, which is consistent with previous studies and clinical experience [46,137,144,184]. The geometric opening area of the 25 mm porcine and bovine aortic valves was 44% and 33% larger than that of the 19 mm valves, respectively [185] (Figure 11). This fact contradicts studies in which there were no differences in survival between the two types of aortic bioprostheses [186,187].

3.4. Multi-Scale Modeling

Significant progress was made in the numerical modeling of heart valves at various scales (tissue and cellular). Models of the interaction between fluid and solid body structure for the movement of the heart valve were developed, which makes it possible to predict the functioning of the valve in the systolic and diastolic phases of the cardiac cycle [39,41,188].
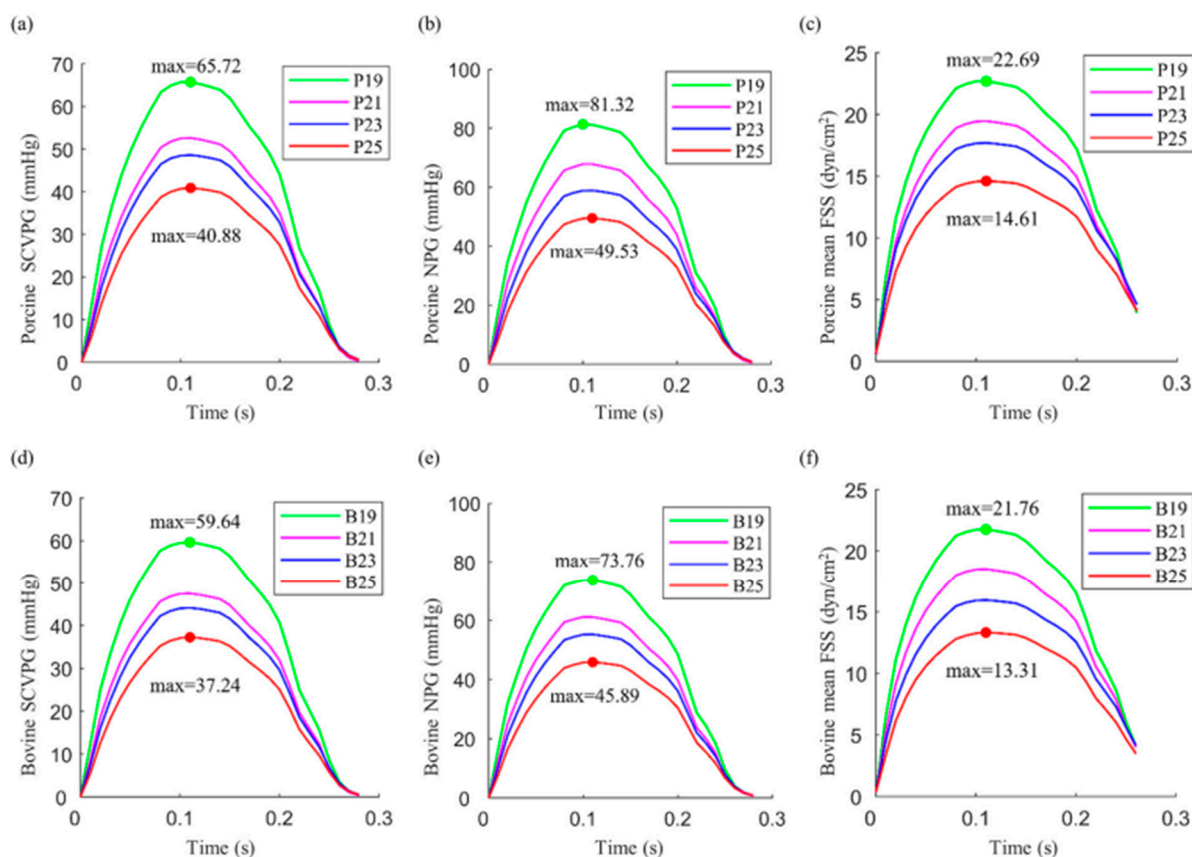
Figure 11. The SCVPG, NPG and mean FSS on the leaflets during systolic phase were obtained from FSI simulations. (**a**,**d**) were SCVPG for porcine and bovine model, respectively. (**b**,**e**) were NPG for porcine and bovine model, respectively. (**c**,**f**) were mean FSS for porcine and bovine model, respectively [37].

In tissue-level modeling, much effort was recently made to formulate and implement digital models consistent with the acquired data [42,88]. In cellular modeling, some results that are associated with experimental data were also obtained [189,190].

It was observed that the wrinkled structure of fibrous tissue serves to protect the tissue and cells within from increased stress. Thus, when large strains are observed in an organ-scale bicuspid valve, they are not transferred to the level of tissues or cells in the region of interest. Therefore, it can be assumed that the difference in calcification is not due to a difference in mechanical deformation [38].

Also, for the organ-scale model, the velocity fields for the bicuspid and tricuspid valves were constructed. Two major differences were observed between tricuspid and bicuspid valves. First, the leaflets of a bicuspid valve do not open as smoothly and are more subjected to flexure. Secondly, the bicuspid valve does not open as wide, and the blood passing through the valve in the systolic phase forms a narrower jet with a less uniform distribution of flow velocity in the cross-section.

3.5. Ozaki Procedure Modeling

Numerical modeling methods are also used to predict the outcome of Ozaki surgery. In [116], the performance of a diseased aortic valve, a normal aortic valve, and three options of corrected diseased aortic valve was modeled and compared using the Ozaki procedure, varying the direction of the fibers in the leaflet substitute relative to its circumferential direction. Figure 12 shows the AV reconstruction model.
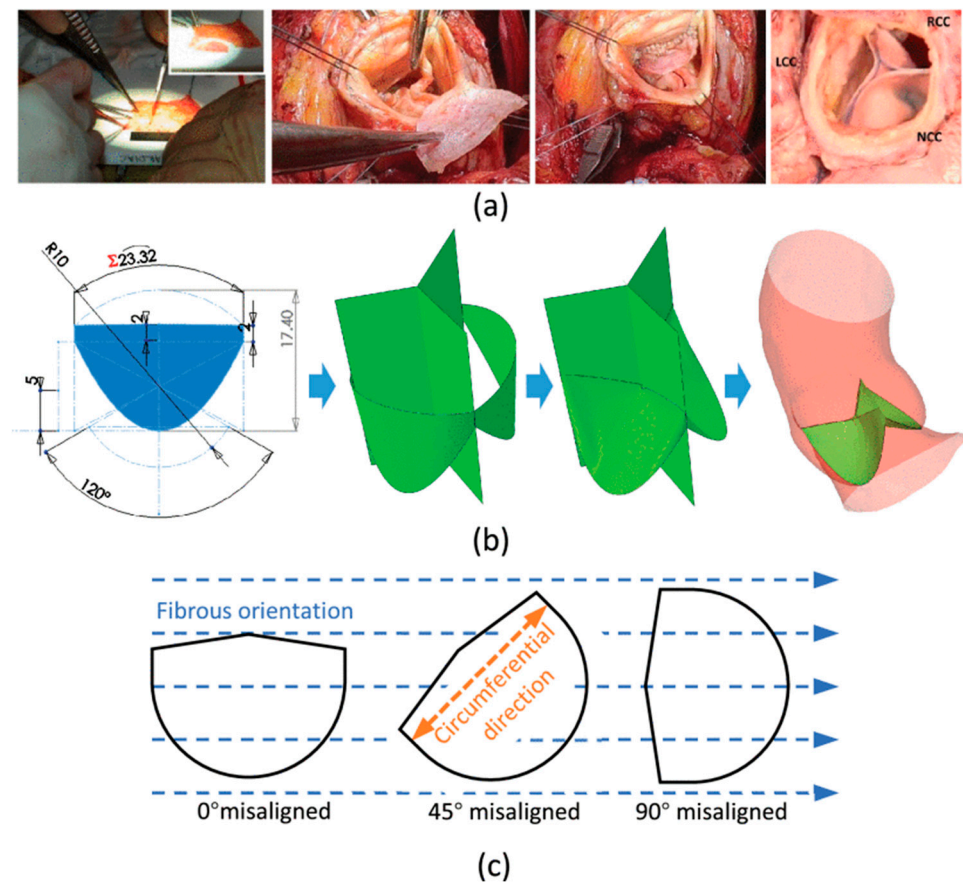
Figure 12. (**a**) Surgical reconstruction of the aortic valve; (**b**) simulated operation on AVNeo; (**c**) illustration of the discrepancy between the circumferential direction of the substitute and the internal orientation of the pericardial fibers [129].

The models allowed researchers to estimate and compare the effective orifice area, the distribution of blood flow velocities, and leaflet stress and strain in five different cases. The study showed that the Ozaki operation on the affected AV can have high clinical effectiveness despite the fact that the direction of the fibers in the autologous pericardium, which acts as a substitute for native leaflets, does not affect the kinematic and hemodynamic characteristics of the reconstructed valve [129].

3.6. Numerical Modeling of a Bileaflet Mechanical Valve

Numerical studies of the mechanical valve have also made several important discoveries: for example, a study was published in which a bicuspid valve was implanted for the first time in an anatomical geometry including its aortic root, ascending and descending aorta, and aortic arch with its main branches (Figure 13). The simulation results were also compared with a model excluding the mobile valve geometry, and the importance of the model with concentrated parameters for the output boundary condition was analyzed. The proposed numerical model and protocol were found to be suitable for performing virtual surgeries with the real geometry of the patient's vascular network, which will help physicians predict the results of future surgery [191].
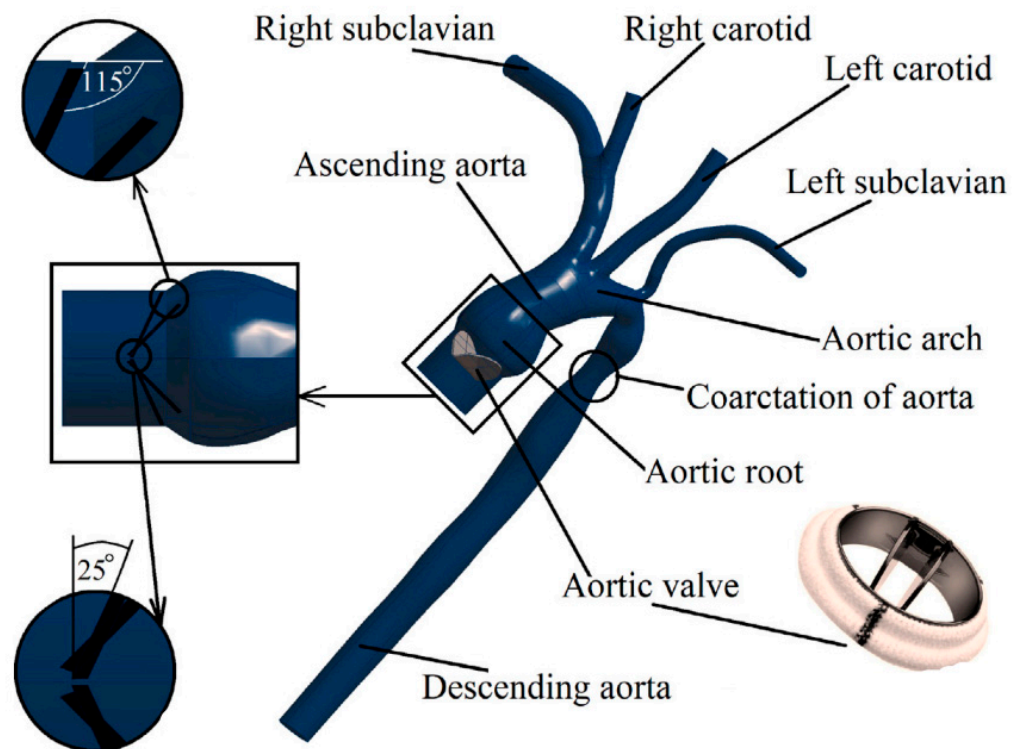
Figure 13. Numerical geometry of the aorta with valve and subsequent branches [191].

It was also proved that the orientation of the valve does not significantly affect the distribution of shear in the ascending aorta, as well as the symmetric closure and minimal rebound of the flaps, which contradicts the study conducted by Borazjani et al. [192]; the 0-degree orientation showed less asymmetry and rebound—factors that are important parameters in determining the amount of intermittent regurgitation [193,194].

4. Discussion

FSI (fluid–structure interaction) simulation of the aortic valve is a computational technique that combines computational fluid dynamics (CFD) and structural mechanics to analyze the behavior of the aortic valve under fluid flow conditions [155,195,196]. FSI and CFD applications are widely used in biomedical engineering [121,197–200].

In this simulation, the aortic valve is typically modeled as a thin elastic structure, while the blood flow through the valve is modeled using the Navier–Stokes equations to capture the fluid dynamics [201–203]. The FSI simulation takes into account the interaction between the fluid and the valve structure, allowing for a more realistic representation of the valve's behavior [204,205].

Estimating the fluid forces acting on the valve leaflets during the cardiac cycle is a crucial component of the FSI simulation [206]. These forces, which are used to predict the deformation of the valve leaflets and the ensuing changes in the flow pattern, are computed based on the fluid velocity, pressure, and viscosity [206,207].

The FSI simulation can provide valuable insights into the functioning of the aortic valve, including the opening and closing dynamics, the stress and strain distribution on the valve leaflets, and the flow characteristics within the valve and downstream in the aorta. It can also be used to study the impact of different pathologies, such as calcification or valve stenosis, on the valve function [208].

Overall, the FSI simulation of the aortic valve is a powerful tool for understanding the fluid–structure interactions in the cardiovascular system and can help in the design of better treatments for valve diseases.

There are several paths open to scientists for further perspectives in development: many researchers take prefabricated valves in the study, while geometry plays a major role. Additionally, the relationship between kinetic energy and spirality in the hemodynamics of prosthetic valves has not been studied; also, the postoperative ventricular hemodynamics of aortic valve replacement with bioprostheses has not been sufficiently studied (or studied superficially), and there may be other variants of bioprostheses. The mechanical valve has not been studied enough because most of the mechanical valves have not been studied.

5. Conclusions

This systematic review is devoted to the structure, main types of dysfunctions, and comprehensive numerical modeling of the aortic valve and can be useful for choosing methods when planning further research in this area. The sources used were selected according to two main types—the literature on aortic valves and literature on computational modeling methods in problems related to heart valves and heart diseases. The main conclusions of this review are as follows:

The two main diseases of the aortic valve are aortic stenosis and aortic insufficiency; the classic surgical correction technique in this case is the replacement of a non-functioning aortic valve (patient's valve) with a valve prosthesis, which can be mechanical, biological, or made from the patient's own pericardium.

Computational modeling is now widely used to study and model complex clinical practice problems.

The main problem in such calculations is the instability of the adaptive algorithm, the high cost of calculations, and the lack of medical data.

New parameters are constantly added when modeling, which is worth paying attention to. Previously, the mechanics of the leaflets were often considered, but now it is necessary to note the distribution of pressure on the surface of the leaflets, the balance of the momentum of the flow, and the dynamics of turbulations when aorta curves.

In most studies, the boundary conditions are specified in the form of pressure at the entrance and output.

Numerical computations of the Ozaki procedure are not yet reproduced on a non-individual scale since the reconstruction technique is considered to be relatively new.

Table 2 below summarizes the main conclusions for the numerical modeling sections of the article.

Table 2. Short summaries.

Section	Summary
Numerical modeling during transplant valve implantation	- the basis for modeling the TAVI operation was created; - computer models were created for patients specifically, what can be used by surgeons when planning the transcatheter implantation procedure; - computed stress distributions give more information about the rupture of the root of the aorta; - was shown that by changing the geometry of the lobes, the stress on the flaps and the model stent is reduced.
Numerical modeling for comparing porcine and bovine aortic valves	- conventional patient assessment and access to the personalized computational framework proposed here might play an important role in predicting and quantifying potential outcomes when different treatment options are available in borderline cases, thus adding further useful information to the clinical decision-making process.

Table 2. *Cont.*

Section	Summary
Modeling at different scales of an organ	- It became possible to predict the functioning of the valve in the systolic and diastolic phases of the heart cycle; - no connection was found between the degree of calcification of the valve and the level of mechanical deformation; - the cusps of the bicuspid valve open less widely, less smoothly, and undergo more bending; Blood, passing through a bicuspid valve into the systolic phase, forms a narrower stream with a less even distribution of flow velocity in the cross-section.
Ozaki procedure modeling	- An individual model of the aortic root after the Ozaki operation was reproduced, which allows the evaluation of the clinical effectiveness of the operation; - The simulation results proved that the direction of fibers in the autologous pericardium does not affect the hemodynamics of the valve after surgery.
Numerical modeling of a bileaflet mechanical valve	- Bicuspid valve implanted for the first time in anatomically volumetric geometry; - Studies have shown that valve orientation has no significant effect on the distribution of viscous shear stress in the ascending aorta.

Conflicts of Interest: The authors declare no conflict of interest.

References

1. Marom, G. Numerical Methods for Fluid–Structure Interaction Models of Aortic Valves. *Arch. Comput. Methods Eng.* **2015**, *22*, 595–620. [CrossRef]
2. Yacoub, M.H.; Takkenberg, J.J.M. Will Heart Valve Tissue Engineering Change the World? *Nat. Clin. Pract. Cardiovasc. Med.* **2005**, *2*, 60–61. [CrossRef]
3. Li, K.Y.C. Bioprosthetic Heart Valves: Upgrading a 50-Year Old Technology. *Front. Cardiovasc. Med.* **2019**, *6*, 47. [CrossRef]
4. Iung, B.; Vahanian, A. Epidemiology of Valvular Heart Disease in the Adult. *Nat. Rev. Cardiol.* **2011**, *8*, 162–172. [CrossRef] [PubMed]
5. Dangas, G.D.; Weitz, J.I.; Giustino, G.; Makkar, R.; Mehran, R. Prosthetic Heart Valve Thrombosis. *J. Am. Coll. Cardiol.* **2016**, *68*, 2670–2689. [CrossRef]
6. Pogosova, G.V.; Oganov, R.G.; Saner, H. Positive Trends in Cardiovascular Mortality in Russia and Moscow: Potential Confounders. *Eur. Heart J.* **2016**, *37*, 3184–3185. [CrossRef]

7. Lakunchykova, O.; Averina, M.; Wilsgaard, T.; Watkins, H.; Malyutina, S.; Ragino, Y.; Keogh, R.H.; Kudryavtsev, A.V.; Govorun, V.; Cook, S.; et al. Why Does Russia Have Such High Cardiovascular Mortality Rates? Comparisons of Blood-Based Biomarkers with Norway Implicate Non-Ischaemic Cardiac Damage. *J. Epidemiol. Community Health* **2020**, *74*, 698–704. [CrossRef]

8. Han, L.; Zhao, S.; Li, S.; Gu, S.; Deng, X.; Yang, L.; Ran, J. Excess Cardiovascular Mortality across Multiple COVID-19 Waves in the United States from March 2020 to March 2022. *Nat. Cardiovasc. Res.* **2023**, *2*, 322–333. [CrossRef]

9. Kamaltdinov, M.R.; Kuchumov, A.G. Application of a mathematical model of systemic circulation for determination of blood flow parameters after modified blalock-taussig shunt operation in newborns. *Russ. J. Biomech.* **2021**, *25*, 268–284.

10. Kamaltdinov, M.; Trusov, P.; Zaitseva, N. A Mathematical Model of the Multiphase Flow in the Antroduodenum: Consideration of the Digestive Enzymes and Regulation Processes. *Ser. Biomech.* **2018**, *32*, 36–42.

11. Kamaltdinov, M.; Trusov, P.; Zaitseva, N. A Multiphase Flow in the Antroduodenum: Some Results of the Mathematical Modelling and Computational Simulation. *MATEC Web Conf.* **2018**, *145*, 04002. [CrossRef]

12. Kuchumov, A.; Tuktamyshev, V.; Kamaltdinov, M. Peristaltic Flow of Lithogenic Bile in the Vateri's Papilla as Non-Newtonian Fluid in the Finite-Length Tube: Analytical and Numerical Results for Reflux Study and Optimization. *Lek. A Technol.* **2017**, *47*, 35–42.

13. Kuchumov, A.G.; Kamaltdinov, M.; Selyaninov, A.; Samartsev, V. Numerical Simulation of Biliary Stent Clogging. *Ser. Biomech.* **2019**, *33*, 3–15.

14. Mantskava, M.M.; Nyashin, Y.I.; Lokhov, V.A. The Study of Blood Circulation at Experimental Tumur Paraneoplasticism. *Russ. J. Biomech.* **2020**, *23*, 505–509.

15. Nowak, M.; Divo, E.; Adamczyk, W.P. Fluid–Structure Interaction Methods for the Progressive Anatomical and Artificial Aortic Valve Stenosis. *Int. J. Mech. Sci.* **2022**, *227*, 107410. [CrossRef]

16. Kuchumov, A.G.; Selyaninov, A. Application of Computational Fluid Dynamics in Biofluids Simulation to Solve Actual Surgery Tasks. *Adv. Intell. Syst. Comput.* **2020**, *1018*, 576–580. [CrossRef]

17. Kuchumov, A. Patient-Specific Bile Flow Simulation to Evaluate Cholecystectomy Outcome. *IOP Conf. Ser. Mater. Sci. Eng.* **2019**, *581*, 012022. [CrossRef]

18. Kuchumov, A. Biomechanical Modelling of Bile Flow in the Biliary System. In Proceedings of the MATEC Web of Conferences, 9 January 2018; Vassilev, V.M., Nikolov, S.G., Datcheva, M.D., Ivanova, Y.P., Eds.; EDP Sciences: Les Ulis, France, 2018; Volume 145, p. 04004.

19. Kuchumov, A.G. Mathematical Modeling of the Peristaltic Lithogenic Bile Flow through the Duct at Papillary Stenosis as a Tapered Finite-Length Tube. *Russ. J. Biomech.* **2016**, *20*, 77–96.

20. Kuchumov, A.G. Biomechanical Model of Bile Flow in the Biliary System. *Russ. J. Biomech.* **2019**, *23*, 224–248.

21. Wu, M.C.H.; Muchowski, H.M.; Johnson, E.L.; Rajanna, M.R.; Hsu, M.C. Immersogeometric Fluid–Structure Interaction Modeling and Simulation of Transcatheter Aortic Valve Replacement. *Comput. Methods Appl. Mech. Eng.* **2019**, *357*, 112556. [CrossRef]

22. Bosi, G.M.; Capelli, C.; Cheang, M.H.; Delahunty, N.; Mullen, M.; Taylor, A.M.; Schievano, S. Population-Specific Material Properties of the Implantation Site for Transcatheter Aortic Valve Replacement Finite Element Simulations. *J. Biomech.* **2018**, *71*, 236–244. [CrossRef]

23. Amindari, A.; Kırkköprü, K.; Saltık, İ.L.; Sünbüloğlu, E. Effect of Non-Linear Leaflet Material Properties on Aortic Valve Dynamics-a Coupled Fluid-Structure Approach. *Eng. Solid Mech.* **2021**, *9*, 123–136. [CrossRef]

24. Mao, W.; Wang, Q.; Kodali, S.; Sun, W. Numerical Parametric Study of Paravalvular Leak Following a Transcatheter Aortic Valve Deployment into a Patient-Specific Aortic Root. *J. Biomech. Eng.* **2018**, *140*, 101007. [CrossRef]

25. Sturla, F.; Votta, E.; Stevanella, M.; Conti, C.A.; Redaelli, A. Impact of modeling fluid–structure interaction in the computational analysis of aortic root biomechanics. *Med. Eng. Phys.* **2013**, *35*, 1721–1730. [CrossRef]

26. Wu, W.; Pott, D.; Mazza, B.; Sironi, T.; Dordoni, E.; Chiastra, C.; Petrini, L.; Pennati, G.; Dubini, G.; Steinseifer, U.; et al. Fluidstructure interaction model of a percutaneous aortic valve: Comparison with an in vitro test and feasibility study in a patient-specific case. *Ann. Biomed. Eng.* **2016**, *44*, 590–603. [CrossRef]

27. Kalyana Sundaram, G.B.; Balakrishnan, K.R.; Kumar, R.K. Aortic Valve Dynamics Using a Fluid Structure Interaction Model-The Physiology of Opening and Closing. *J. Biomech.* **2015**, *48*, 1737–1744. [CrossRef]

28. Tzamtzis, S.; Viquerat, J.; Yap, J.; Mullen, M.J.; Burriesci, G. Numerical Analysis of the Radial Force Produced by the Medtronic-CoreValve and Edwards-SAPIEN after Transcatheter Aortic Valve Implantation (TAVI). *Med. Eng. Phys.* **2013**, *35*, 125–130. [CrossRef] [PubMed]

29. Bosmans, B.; Famaey, N.; Verhoelst, E.; Bosmans, J.; Vander Sloten, J. A Validated Methodology for Patient Specific Computational Modeling of Self-Expandable Transcatheter Aortic Valve Implantation. *J. Biomech.* **2016**, *49*, 2824–2830. [CrossRef] [PubMed]

30. Finotello, A.; Morganti, S.; Auricchio, F. Finite Element Analysis of TAVI: Impact of Native Aortic Root Computational Modeling Strategies on Simulation Outcomes. *Med. Eng. Phys.* **2017**, *47*, 2–12. [CrossRef] [PubMed]

31. Wang, Q.; Kodali, S.; Primiano, C.; Sun, W. Simulations of Transcatheter Aortic Valve Implantation: Implications for Aortic Root Rupture. *Biomech. Model. Mechanobiol.* **2015**, *14*, 29–38. [CrossRef]

32. Dowling, C.; Bavo, A.M.; El Faquir, N.; Mortier, P.; De Jaegere, P.; De Backer, O.; Sondergaard, L.; Ruile, P.; Mylotte, D.; McConkey, H.; et al. Patient-Specific Computer Simulation of Transcatheter Aortic Valve Replacement in Bicuspid Aortic Valve Morphology. *Circ. Cardiovasc. Imaging* **2019**, *12*, e009178. [CrossRef] [PubMed]

33.　Bianchi, M.; Marom, G.; Ghosh, R.P.; Rotman, O.M.; Parikh, P.; Gruberg, L.; Bluestein, D. Patient-Specific Simulation of Transcatheter Aortic Valve Replacement: Impact of Deployment Options on Paravalvular Leakage. *Biomech. Model. Mechanobiol.* **2019**, *18*, 435–451. [CrossRef] [PubMed]

34.　Whelan, A.; Duffy, J.; Gaul, R.T.; O'Reilly, D.; Nolan, D.R.; Gunning, P.; Lally, C.; Murphy, B.P. Collagen fibre orientation and dispersion govern ultimate tensile strength, stiffness and the fatigue performance of bovine pericardium. *J. Mech. Behav Biomed Mater.* **2019**, *90*, 54–60. [CrossRef]

35.　Travaglino, S.; Murdock, K.; Tran, A.; Martin, C.; Liang, L.; Wang, Y.; Sun, W. Computational Optimization Study of Transcatheter Aortic Valve Leaflet Design Using Porcine and Bovine Leaflets. *J. Biomech. Eng.* **2020**, *142*, 011007. [CrossRef]

36.　van Loon, R.; Anderson, P.D.; de Hart, J.; Baaijens, F.P.T. A Combined Fictitious Domain/Adaptive Meshing Method for Fluid-Structure Interaction in Heart Valves. *Int. J. Numer. Methods Fluids* **2004**, *46*, 533–544. [CrossRef]

37.　Li, C.; Tang, D.; Yao, J.; Shao, Y.; Sun, H.; Hammer, P.; Gong, C.; Ma, L.; Zhang, Y.; Wang, L.; et al. Porcine and Bovine Aortic Valve Comparison for Surgical Optimization: A Fluid-Structure Interaction Modeling Study. *Int. J. Cardiol.* **2021**, *334*, 88–95. [CrossRef]

38.　Weinberg, E.J.; Kaazempur Mofrad, M.R. A Multiscale Computational Comparison of the Bicuspid and Tricuspid Aortic Valves in Relation to Calcific Aortic Stenosis. *J. Biomech.* **2008**, *41*, 3482–3487. [CrossRef]

39.　De Hart, J.; Peters, G.W.M.; Schreurs, P.J.G.; Baaijens, F.P.T. A Three-Dimensional Computational Analysis of Fluid-Structure Interaction in the Aortic Valve. *J. Biomech.* **2003**, *36*, 103–112. [CrossRef]

40.　Nicosia, M.A.; Cochran, R.P.; Einstein, D.R.; Rutland, C.J.; Kunzelman, K.S. A coupled fluid-structure finite element model of the aortic valve and root. *J. Heart Valve Dis.* **2003**, *12*, 781–789.

41.　Weinberg, E.J.; Kaazempur-Mofrad, M.R. On the Constitutive Models for Heart Valve Leaflet Mechanics. *Cardiovasc. Eng.* **2005**, *5*, 37–43. [CrossRef]

42.　Stella, J.A.; Sacks, M.S. On the Biaxial Mechanical Properties of the Layers of the Aortic Valve Leaflet. *J. Biomech. Eng.* **2007**, *129*, 757–766. [CrossRef]

43.　Weinberg, E.J.; Kaazempur Mofrad, M.R. A Finite Shell Element for Heart Mitral Valve Leaflet Mechanics, with Large Deformations and 3D Constitutive Material Model. *J. Biomech.* **2007**, *40*, 705–711. [CrossRef] [PubMed]

44.　Liu, X.; Zhang, W.; Ye, P.; Luo, Q.; Chang, Z. Fluid-Structure Interaction Analysis on the Influence of the Aortic Valve Stent Leaflet Structure in Hemodynamics. *Front. Physiol.* **2022**, *13*, 904453. [CrossRef]

45.　Pil, N.; Kuchumov, A.G.; Kadyraliev, B.; Arutunyan, V. Influence of Aortic Valve Leaflet Material Model on Hemodynamic Features in Healthy and Pathological States. *Mathematics* **2023**, *11*, 428. [CrossRef]

46.　Qashqaie Abdi, S.; Hassani, K. The Study of the Relationship between Unicuspid Aortic Valve Insufficiency and Heart Disease by Fluid-Structure Interaction Modeling. *Biomed. Eng. Adv.* **2023**, *5*, 100079. [CrossRef]

47.　Bosi, G.M.; Capelli, C.; Cheang, M.H.; Delahunty, N.; Mullen, M.; Taylor, A.M.; Schievano, S. A validated computational framework to predict outcomes in TAVI. *Sci. Rep.* **2020**, *10*, 9906. [CrossRef]

48.　Morany, A.; Lavon, K.; Gomez Bardon, R.; Kovarovic, B.; Hamdan, A.; Bluestein, D.; Haj-Ali, R. Fluid–Structure Interaction Modeling of Compliant Aortic Valves Using the Lattice Boltzmann CFD and FEM Methods. *Biomech. Model. Mechanobiol.* **2023**, *22*, 837–850. [CrossRef]

49.　Hinton, R.B.; Yutzey, K.E. Heart Valve Structure and Function in Development and Disease. *Annu. Rev. Physiol.* **2011**, *73*, 29–46. [CrossRef]

50.　Zamorano, J.L.; Gonçalves, A.; Lang, R. Imaging to Select and Guide Transcatheter Aortic Valve Implantation. *Eur. Heart J.* **2014**, *35*, 1578–1587. [CrossRef]

51.　Paiocchi, V.L.; Faletra, F.F.; Ferrari, E.; Schlossbauer, S.A.; Leo, L.A.; Maisano, F. Multimodality Imaging of the Anatomy of the Aortic Root. *J. Cardiovasc. Dev. Dis.* **2021**, *8*, 51. [CrossRef]

52.　Loukas, M.; Bilinsky, E.; Bilinsky, S.; Blaak, C.; Tubbs, R.S.; Anderson, R.H. The Anatomy of the Aortic Root. *Clin. Anat.* **2014**, *27*, 748–756. [CrossRef] [PubMed]

53.　Edwards, J.E. Pathology of left ventricular outflow tract obstruction. *Circulation* **1965**, *31*, 586–599. [CrossRef] [PubMed]

54.　Redel, D.A. Blood Flow Velocity Patterns in Heart Disease. In *Color Blood Flow Imaging of the Heart*; Springer: Berlin, Heidelberg, 1988.

55.　Suvorov, V.V.; Fedotova, E.P.; Zaitsev, V.V.; Dolgova, E.V.; Popova, L.L.; Glazunova, A.E.; Novak, M.U.; Nasyrov, R.A. A Rare Case of Diagnosed Absent Aortic Valve and Severely Hypoplastic Pulmonary Valve with Double Outlet Right Ventricle: A Case Report. *Heliyon* **2023**, *9*, e17373. [CrossRef] [PubMed]

56.　Naeije, R.; Tello, K.; D'Alto, M. Tricuspid Regurgitation: Right Ventricular Volume Versus Pressure Load. *Curr. Heart. Fail. Rep.* **2023**, *20*, 208–217. [CrossRef]

57.　Prodromo, J.; D'Ancona, G.; Amaducci, A.; Pilato, M. Aortic Valve Repair for Aortic Insufficiency: A Review. *J. Cardiothorac. Vasc. Anesth.* **2012**, *26*, 923–932. [CrossRef]

58.　Reed, A.; Bajwa, S.; Schuh, S.; Mikhael, M. Incidental Perforation of Aortic Valve Leaflet Found on Presentation of Cardiogenic Shock. *Cureus* **2023**, *15*, e39476. [CrossRef]

59.　Sassis, L.; Kefala-Karli, P.; Cucchi, I.; Kouremenos, I.; Demosthenous, M.; Diplaris, K. Valve Repair in Aortic Insufficiency: A State-of-the-Art Review. *Curr. Cardiol. Rev.* **2022**, *19*, 21–31. [CrossRef]

60.　Ziganshin, B.A.; Kargin, N.; Zafar, M.A.; Elefteriades, J.A. The Natural History of Aortic Root Aneurysms. *Ann. Cardiothorac. Surg.* **2023**, *12*, 213–224. [CrossRef]

61. Chung, J.C.-Y. Pathology and Pathophysiology of the Aortic Root. *Ann. Cardiothorac. Surg.* **2023**, *12*, 159–167. [CrossRef]
62. Masri, A.; Kalahasti, V.; Alkharabsheh, S.; Svensson, L.G.; Sabik, J.F.; Roselli, E.E.; Hammer, D.; Johnston, D.R.; Collier, P.; Rodriguez, L.L.; et al. Characteristics and Long-Term Outcomes of Contemporary Patients with Bicuspid Aortic Valves. *J. Thorac. Cardiovasc. Surg.* **2016**, *151*, 1650–1659.e1. [CrossRef]
63. Hoffman, J.I.E.; Kaplan, S. The Incidence of Congenital Heart Disease. *J. Am. Coll. Cardiol.* **2002**, *39*, 1890–1900. [CrossRef]
64. Cripe, L.; Andelfinger, G.; Martin, L.J.; Shooner, K.; Benson, D.W. Bicuspid Aortic Valve Is Heritable. *J. Am. Coll. Cardiol.* **2004**, *44*, 138–143. [CrossRef]
65. Ellison, J.W.; Yagubyan, M.; Majumdar, R.; Sarkar, G.; Bolander, M.E.; Atkinson, E.J.; Sarano, M.E.; Sundt, T.M. Evidence of Genetic Locus Heterogeneity for Familial Bicuspid Aortic Valve. *J. Surg. Res.* **2007**, *142*, 28–31. [CrossRef] [PubMed]
66. Huntington, K.; Hunter, A.G.W.; Chan, K.L. A Prospective Study to Assess the Frequency of Familial Clustering of Congenital Bicuspid Aortic Valve. *J. Am. Coll. Cardiol.* **1997**, *30*, 1809–1812. [CrossRef] [PubMed]
67. Mcdonald, K.; Maurer, B.J. Familial Aortic Valve Disease: Evidence for a Genetic Influence? *Eur. Heart J.* **1989**, *10*, 676–677. [CrossRef] [PubMed]
68. Glick, B.N.; Roberts, W.C. Congenitally Bicuspid Aortic Valve in Multiple Family Members. *Am. J. Cardiol.* **1994**, *73*, 400–404. [CrossRef]
69. Della Corte, A.; Bancone, C.; Quarto, C.; Dialetto, G.; Covino, F.E.; Scardone, M.; Caianiello, G.; Cotrufo, M. Predictors of Ascending Aortic Dilatation with Bicuspid Aortic Valve: A Wide Spectrum of Disease Expression. *Eur. J. Cardio-Thorac. Surg.* **2007**, *31*, 397–405. [CrossRef]
70. Emanuel, R.; Withers, R.; O'Brien, K.; Ross, P.; Feizi, Ö. Congenitally Bicuspid Aortic Valves. Clinicogenetic Study of 41 Families. *Heart* **1978**, *40*, 1402–1407. [CrossRef] [PubMed]
71. Otto, C.M. Calcification of Bicuspid Aortic Valves. *Heart* **2002**, *88*, 321–322. [CrossRef]
72. Lewin, M.B.; Otto, C.M. The Bicuspid Aortic Valve: Adverse Outcomes from Infancy to Old Age. *Circulation* **2005**, *111*, 832–834. [CrossRef]
73. Slama, M.; Tribouilloy, C.; Maizel, J. Left Ventricular Outflow Tract Obstruction in ICU Patients. *Curr. Opin. Crit. Care* **2016**, *22*, 260–266. [CrossRef] [PubMed]
74. Joseph, J.; Naqvi, S.Y.; Giri, J.; Goldberg, S. Aortic Stenosis: Pathophysiology, Diagnosis, and Therapy. *Am. J. Med.* **2017**, *130*, 253–263. [CrossRef] [PubMed]
75. Mas-Peiro, S.; Fichtlscherer, S.; Walther, C.; Vasa-Nicotera, M. Current Issues in Transcatheter Aortic Valve Replacement. *J. Thorac. Dis.* **2020**, *12*, 1665–1680. [CrossRef]
76. Nathaniel, S. Aortic Stenosis: An Update. *World J. Cardiol.* **2010**, *2*, 135–139. [CrossRef]
77. Boskovski, M.T.; Gleason, T.G. Current Therapeutic Options in Aortic Stenosis. *Circ. Res.* **2021**, *128*, 1398–1417. [CrossRef] [PubMed]
78. Marijon, E.; Mirabel, M.; Celermajer, D.S.; Jouven, X. Rheumatic Heart Disease. *Lancet* **2012**, *379*, 953–964. [CrossRef] [PubMed]
79. Choudhary, S.K.; Talwar, S.; Airan, B. Choice of Prosthetic Heart Valve in a Developing Country. *Heart Asia* **2016**, *8*, 65–72. [CrossRef]
80. Rasheed, N.F.; Stonebraker, C.; Li, Z.; Siddiqi, U.; Lee, A.C.H.; Li, W.; Lupo, S.; Cruz, J.; Cohen, W.G.; Staub, C.; et al. Figure of Eight Suture Technique in Aortic Valve Replacement Decreases Prosthesis-Patient Mismatch. *J. Cardiothorac. Surg.* **2023**, *18*, 117. [CrossRef] [PubMed]
81. Head, S.J.; Çelik, M.; Kappetein, A.P. Mechanical versus Bioprosthetic Aortic Valve Replacement. *Eur. Heart J.* **2017**, *38*, 2183–2191. [CrossRef]
82. Pibarot, P.; Dumesnil, J.G. Prosthetic Heart Valves: Selection of the Optimal Prosthesis and Long-Term Management. *Circulation* **2009**, *119*, 1034–1048. [CrossRef]
83. Ascione, G.; Denti, P. Transcatheter Mitral Valve Replacement and Thrombosis: A Review. *Front. Cardiovasc. Med.* **2021**, *8*, 621258. [CrossRef]
84. Babur Guler, G.; Memic Sancar, K.; Corekcioglu, B.; Topel, C.; Erturk, M. Early Valve Thrombosis Management after Successful Transcatheter Tricuspid Valve-in-Valve Implantation. *JACC Case Rep.* **2023**, *5*, 101584. [CrossRef]
85. Couper, G.S. Surgical Aspects of Prosthetic Valve Selection. In *Overview of Cardiac Surgery for the Cardiologist*; Springer: New York, NY, USA, 1994.
86. Russo, M.; Taramasso, M.; Guidotti, A.; Pozzoli, A.; Nietilspach, F.; von Segesser, L.K.; Maisano, F. The Evolution of Surgical Valves. *Cardiovasc. Med.* **2017**, *20*, 285–292. [CrossRef]
87. Lund, O.; Nielsen, S.L.; Arildsen, H.; Ilkjaer, L.B.; Pilegaard, H.K. Standard Aortic St. Jude Valve at 18 Years: Performance Profile and Determinants of Outcome. *Ann. Thorac. Surg.* **2000**, *69*, 1459–1465. [CrossRef] [PubMed]
88. Sacks, M.S.; Yoganathan, A.P. Heart Valve Function: A Biomechanical Perspective. *Philos. Trans. R. Soc. B Biol. Sci.* **2007**, *362*, 1369–1391. [CrossRef] [PubMed]
89. Ashour, Z.A.; Shawky, H.A.F.; Hussein, M.H. Outcome of Pregnancy in Women with Mechanical Valves. *Tex. Heart Inst. J.* **2000**, *27*, 240–245. [PubMed]
90. Ng, A.P.; Verma, A.; Sanaiha, Y.; Williamson, C.G.; Afshar, Y.; Benharash, P. Maternal and Fetal Outcomes in Pregnant Patients with Mechanical and Bioprosthetic Heart Valves. *J. Am. Heart Assoc.* **2023**, *12*, e028653. [CrossRef] [PubMed]
91. Jaffer, I.H.; Whitlock, R.P. A Mechanical Heart Valve Is the Best Choice. *Heart Asia* **2016**, *8*, 62–64. [CrossRef] [PubMed]

92. Siddiqui, R.F.; Abraham, J.R.; Butany, J. Bioprosthetic Heart Valves: Modes of Failure. *Histopathology* **2009**, *55*, 135–144. [CrossRef]

93. Blum, K.M.; Drews, J.D.; Breuer, C.K. Tissue-Engineered Heart Valves: A Call for Mechanistic Studies. *Tissue Eng. Part B Rev.* **2018**, *24*, 240–253. [CrossRef] [PubMed]

94. Meuris, B.; De Praetere, H.; Strasly, M.; Trabucco, P.; Lai, J.C.; Verbrugghe, P.; Herijgers, P. A Novel Tissue Treatment to Reduce Mineralization of Bovine Pericardial Heart Valves. *J. Thorac. Cardiovasc. Surg.* **2018**, *156*, 197–206. [CrossRef] [PubMed]

95. Williams, D.F.; Bezuidenhout, D.; de Villiers, J.; Human, P.; Zilla, P. Long-Term Stability and Biocompatibility of Pericardial Bioprosthetic Heart Valves. *Front. Cardiovasc. Med.* **2021**, *8*, 728577. [CrossRef]

96. Campion, G.; Hershberger, K.; Whelan, A.; Conroy, J.; Lally, C.; Murphy, B.P. A Biomechanical and Microstructural Analysis of Bovine and Porcine Pericardium for Use in Bioprosthetic Heart Valves. *Struct. Heart* **2021**, *5*, 486–496. [CrossRef]

97. Soares, J.S.; Feaver, K.R.; Zhang, W.; Kamensky, D.; Aggarwal, A.; Sacks, M.S. Biomechanical Behavior of Bioprosthetic Heart Valve Heterograft Tissues: Characterization, Simulation, and Performance. *Cardiovasc. Eng. Technol.* **2016**, *7*, 309–351. [CrossRef] [PubMed]

98. Kostyunin, A.E.; Yuzhalin, A.E.; Rezvova, M.A.; Ovcharenko, E.A.; Glushkova, T.V.; Kutikhin, A.G. Degeneration of Bioprosthetic Heart Valves: Update 2020. *J. Am. Heart Assoc.* **2020**, *9*, e018506. [CrossRef] [PubMed]

99. Ciolacu, D.E.; Nicu, R.; Ciolacu, F. Natural Polymers in Heart Valve Tissue Engineering: Strategies, Advances and Challenges. *Biomedicines* **2022**, *10*, 1095. [CrossRef]

100. Kalogeropoulos, A.S.; Redwood, S.R.; Allen, C.J.; Hurrell, H.; Chehab, O.; Rajani, R.; Prendergast, B.; Patterson, T. A 20-Year Journey in Transcatheter Aortic Valve Implantation: Evolution to Current Eminence. *Front. Cardiovasc. Med.* **2022**, *9*, 971762. [CrossRef]

101. Nappi, F.; Singh, S.S.A.; Nappi, P.; Fiore, A. Biomechanics of Transcatheter Aortic Valve Implant. *Bioengineering* **2022**, *9*, 299. [CrossRef]

102. Rotman, O.M.; Bianchi, M.; Ghosh, R.P.; Kovarovic, B.; Bluestein, D. Principles of TAVR Valve Design, Modelling, and Testing. *Expert Rev. Med. Devices* **2018**, *15*, 771–791. [CrossRef]

103. Kilic, T.; Yilmaz, I. Transcatheter Aortic Valve Implantation: A Revolution in the Therapy of Elderly and High-Risk Patients with Severe Aortic Stenosis. *J. Geriatr. Cardiol.* **2017**, *14*, 204–217.

104. Tamburino, C.; Valvo, R.; Crioscione, E.; Reddavid, C.; Picci, A.; Costa, G.; Barbanti, M. The Path of Transcatheter Aortic Valve Implantation: From Compassionate to Low-Risk Cases. *Eur. Heart J. Suppl.* **2020**, *22*, L140–L145. [CrossRef] [PubMed]

105. Mitsis, A.; Yuan, X.; Eftychiou, C.; Avraamides, P.; Nienaber, C.A. Personalised Treatment in Aortic Stenosis: A Patient-Tailored Transcatheter Aortic Valve Implantation Approach. *J. Cardiovasc. Dev. Dis.* **2022**, *9*, 407. [CrossRef]

106. Luraghi, G.; Rodriguez Matas, J.F.; Migliavacca, F. In Silico Approaches for Transcatheter Aortic Valve Replacement Inspection. *Expert Rev. Cardiovasc. Ther.* **2021**, *19*, 61–70. [CrossRef] [PubMed]

107. Manji, R.A.; Lee, W.; Cooper, D.K.C. Xenograft Bioprosthetic Heart Valves: Past, Present and Future. *Int. J. Surg.* **2015**, *23*, 280–284. [CrossRef]

108. Ruel, M.; Kulik, A.; Lam, B.; Rubens, F.; Hendry, P.; Masters, R.; Bedard, P.; Mesana, T. Long-Term Outcomes of Valve Replacement with Modern Prostheses in Young Adults. *Eur. J. Cardio-Thorac. Surg.* **2005**, *27*, 425–433. [CrossRef] [PubMed]

109. Sulejmani, F.; Caballero, A.; Martin, C.; Pham, T.; Sun, W. Evaluation of Transcatheter Heart Valve Biomaterials: Computational Modeling Using Bovine and Porcine Pericardium. *J. Mech. Behav. Biomed. Mater.* **2019**, *97*, 159–170. [CrossRef] [PubMed]

110. Ozaki, S.; Kawase, I.; Yamashita, H.; Uchida, S.; Takatoh, M.; Kiyohara, N. Midterm Outcomes after Aortic Valve Neocuspidization with Glutaraldehyde-Treated Autologous Pericardium. *J. Thorac. Cardiovasc. Surg.* **2018**, *155*, 2379–2387. [CrossRef]

111. Ozaki, S.; Kawase, I.; Yamashita, H.; Uchida, S.; Takatoh, M.; Hagiwara, S.; Kiyohara, N. Aortic Valve Reconstruction Using Autologous Pericardium for Aortic Stenosis. *Circ. J.* **2015**, *79*, 1504–1510. [CrossRef]

112. Ozaki, S.; Kawase, I.; Yamashita, H.; Uchida, S.; Nozawa, Y.; Takatoh, M.; Hagiwara, S. A Total of 404 Cases of Aortic Valve Reconstruction with Glutaraldehyde-Treated Autologous Pericardium. *J. Thorac. Cardiovasc. Surg.* **2014**, *147*, 301–306. [CrossRef]

113. Saisho, H.; Scharfschwerdt, M.; Schaller, T.; Sadat, N.; Aboud, A.; Ensminger, S.; Fujita, B. Ex Vivo Evaluation of the Ozaki Procedure in Comparison with the Native Aortic Valve and Prosthetic Valves. *Interact. Cardiovasc. Thorac. Surg.* **2022**, *35*, ivac199. [CrossRef]

114. Theodoridis, K.; Müller, J.; Ramm, R.; Findeisen, K.; Andrée, B.; Korossis, S.; Haverich, A.; Hilfiker, A. Effects of Combined Cryopreservation and Decellularization on the Biomechanical, Structural and Biochemical Properties of Porcine Pulmonary Heart Valves. *Acta Biomater.* **2016**, *43*, 71–77. [CrossRef]

115. Hu, X.; Li, S.; Peng, P.; Wang, B.; Liu, W.; Dong, X.; Yang, X.; Karabaliev, M.; Yu, Q.; Gao, C. Prosthetic Heart Valves for Transcatheter Aortic Valve Replacement. *BMEMat* **2023**, *1*, e12026. [CrossRef]

116. Nistal, F.; Garcia-Martinez, V.; Arbe, E.; Fernandez, D.; Artinano, E.; Mazorra, F.; Gallo, I. In Vivo Experimental Assessment of Polytetrafluoroethylene Trileaflet Heart Valve Prosthesis. *J. Thorac. Cardiovasc. Surg.* **1990**, *99*, 1074–1081. [CrossRef]

117. Kütting, M.; Roggenkamp, J.; Urban, U.; Schmitz-Rode, T.; Steinseifer, U. Polyurethane Heart Valves: Past, Present and Future. *Expert Rev. Med. Devices* **2011**, *8*, 227–233. [CrossRef]

118. Singh, S.K.; Kachel, M.; Castillero, E.; Xue, Y.; Kalfa, D.; Ferrari, G.; George, I. Polymeric Prosthetic Heart Valves: A Review of Current Technologies and Future Directions. *Front. Cardiovasc. Med.* **2023**, *10*, 1137827. [CrossRef] [PubMed]

119. Li, R.L.; Russ, J.; Paschalides, C.; Ferrari, G.; Waisman, H.; Kysar, J.W.; Kalfa, D. Mechanical Considerations for Polymeric Heart Valve Development: Biomechanics, Materials, Design and Manufacturing. *Biomaterials* **2019**, *225*, 119493. [CrossRef] [PubMed]

120. Kuchumov, A.G.; Nyashin, Y.I.; Samartsev, V.A. Modelling of Peristaltic Bile Flow in the Papilla Ampoule with Stone and in the Papillary Stenosis Case: Application to Reflux Investigation. *IFMBE Proc.* **2015**, *52*, 158–161.

121. Kuchumov, A.G.; Nyashin, Y.I.; Samarcev, V.A.; Gavrilov, V.A. Modelling of the Pathological Bile Flow in the Duct with a Calculus. *Acta Bioeng. Biomech.* **2013**, *15*, 9–17. [CrossRef] [PubMed]

122. Kuchumov, A.G.; Gilev, V.; Popov, V.; Samartsev, V.; Gavrilov, V. Non-Newtonian Flow of Pathological Bile in the Biliary System: Experimental Investigation and CFD Simulations. *Korea Aust. Rheol. J.* **2014**, *26*, 81–90. [CrossRef]

123. Kuchumov, A.G.; Khairulin, A.; Shmurak, M.; Porodikov, A.; Merzlyakov, A. The Effects of the Mechanical Properties of Vascular Grafts and an Anisotropic Hyperelastic Aortic Model on Local Hemodynamics during Modified Blalock–Taussig Shunt Operation, Assessed Using FSI Simulation. *Materials* **2022**, *15*, 2719. [CrossRef]

124. Kuchumov, A.G.; Vedeneev, V.; Samartsev, V.; Khairulin, A.; Ivanov, O. Patient-Specific Fluid–Structure Interaction Model of Bile Flow: Comparison between 1-Way and 2-Way Algorithms. *Comput. Methods Biomech. Biomed. Eng.* **2021**, *24*, 1693–1717. [CrossRef] [PubMed]

125. Zakerzadeh, R.; Hsu, M.C.; Sacks, M.S. Computational Methods for the Aortic Heart Valve and Its Replacements. *Expert Rev. Med. Devices* **2017**, *14*, 849–866. [CrossRef]

126. Tahir, A.M.; Mutlu, O.; Bensaali, F.; Ward, R.; Ghareeb, A.N.; Helmy, S.M.H.A.; Othman, K.T.; Al-Hashemi, M.A.; Abujalala, S.; Chowdhury, M.E.H.; et al. Latest Developments in Adapting Deep Learning for Assessing TAVR Procedures and Outcomes. *J. Clin. Med.* **2023**, *12*, 4774. [CrossRef]

127. McLoone, M.; Quinlan, N.J. Coupling of the Meshless Finite Volume Particle Method and the Finite Element Method for Fluid–Structure Interaction with Thin Elastic Structures. *Eur. J. Mech. B Fluids* **2022**, *92*, 117–131. [CrossRef]

128. Diniz dos Santos, N.; Gerbeau, J.F.; Bourgat, J.F. A Partitioned Fluid-Structure Algorithm for Elastic Thin Valves with Contact. *Comput. Methods Appl. Mech. Eng.* **2008**, *197*, 1750–1761. [CrossRef]

129. Feng, Y.; Cao, Y.; Wang, W.; Zhang, H.; Wei, L.; Jia, B.; Wang, S. Computational Modeling for Surgical Reconstruction of Aortic Valve by Using Autologous Pericardium. *IEEE Access* **2020**, *8*, 97343–97352. [CrossRef]

130. Fernández, M.A.; Moubachir, M. A Newton Method Using Exact Jacobians for Solving Fluid-Structure Coupling. *Comput. Struct.* **2005**, *83*, 127–142. [CrossRef]

131. Shadden, S.C.; Astorino, M.; Gerbeau, J.F. Computational Analysis of an Aortic Valve Jet with Lagrangian Coherent Structures. *Chaos* **2010**, *20*, 017512. [CrossRef]

132. Cheng, R.; Lai, Y.G.; Chandran, K.B. Three-Dimensional Fluid-Structure Interaction Simulation of Bileaflet Mechanical Heart Valve Flow Dynamics. *Ann. Biomed. Eng.* **2004**, *32*, 1471–1483. [CrossRef]

133. Dumont, K.; Vierendeels, J.; Kaminsky, R.; Van Nooten, G.; Verdonck, P.; Bluestein, D. Comparison of the Hemodynamic and Thrombogenic Performance of Two Bileaflet Mechanical Heart Valves Using a CFD/FSI Model. *J. Biomech. Eng.* **2007**, *129*, 558–565. [CrossRef]

134. Kandail, H.S.; Trivedi, S.D.; Shaikh, A.C.; Bajwa, T.K.; O'Hair, D.P.; Jahangir, A.; LaDisa, J.F. Impact of Annular and Supra-Annular CoreValve Deployment Locations on Aortic and Coronary Artery Hemodynamics. *J. Mech. Behav. Biomed. Mater.* **2018**, *86*, 131–142. [CrossRef]

135. Abbas, S.S.; Nasif, M.S.; Al-Waked, R. State-of-the-Art Numerical Fluid–Structure Interaction Methods for Aortic and Mitral Heart Valves Simulations: A Review. *Simulation* **2022**, *98*, 3–34. [CrossRef]

136. Nejadmalayeri, A.; Hoffmann, K.A.; Dietiker, J.F. Numerical Simulation of Pulsatile Blood Flow across a Tilting-Disk Valve. In Proceedings of the Collection of Technical Papers-37th AIAA Fluid Dynamics Conference, Miami, FL, USA, 25–28 June 2007; Volume 3.

137. De Vita, F.; de Tullio, M.D.; Verzicco, R. Numerical Simulation of the Non-Newtonian Blood Flow through a Mechanical Aortic Valve: Non-Newtonian Blood Flow in the Aortic Root. *Theor. Comput. Fluid Dyn.* **2016**, *30*, 129–138. [CrossRef]

138. Hedayat, M.; Asgharzadeh, H.; Borazjani, I. Platelet Activation of Mechanical versus Bioprosthetic Heart Valves during Systole. *J. Biomech.* **2017**, *56*, 111–116. [CrossRef] [PubMed]

139. Li, W.-Q.; Gao, Z.-X.; Jin, Z.-J.; Qian, J.-Y. Transient Study of Flow and Cavitation inside a Bileaflet Mechanical Heart Valve. *Appl. Sci.* **2020**, *10*, 2548. [CrossRef]

140. Kuan, Y.H.; Kabinejadian, F.; Nguyen, V.T.; Su, B.; Yoganathan, A.P.; Leo, H.L. Comparison of Hinge Microflow Fields of Bileaflet Mechanical Heart Valves Implanted in Different Sinus Shape and Downstream Geometry. *Comput. Methods Biomech. Biomed. Eng.* **2015**, *18*, 1785–1796. [CrossRef]

141. Yun, B.M.; Wu, J.; Simon, H.A.; Arjunon, S.; Sotiropoulos, F.; Aidun, C.K.; Yoganathan, A.P. A Numerical Investigation of Blood Damage in the Hinge Area of Aortic Bileaflet Mechanical Heart Valves during the Leakage Phase. *Ann. Biomed. Eng.* **2012**, *40*, 1468–1485. [CrossRef]

142. Simon, H.A.; Ge, L.; Sotiropoulos, F.; Yoganathan, A.P. Numerical Investigation of the Performance of Three Hinge Designs of Bileaflet Mechanical Heart Valves. *Ann. Biomed. Eng.* **2010**, *38*, 3295–3310. [CrossRef]

143. Abbas, S.S.; Nasif, M.S.; Said, M.A.M.; Al-Waked, R. Numerical Simulation of the Non-Newtonian Blood Flow through Aortic Bileaflet Mechanical Heart Valve Using Fluid-Structure Interaction Approach. In Proceedings of the AIP Conference Proceedings, Kuala Lumpur, Malaysia, 13–14 August 2018; Volume 2035.

144. Dasi, L.P.; Sucosky, P.; De Zelicourt, D.; Sundareswaran, K.; Jimenez, J.; Yoganathan, A.P. Advances in Cardiovascular Fluid Mechanics: Bench to Bedside. *Ann. N. Y. Acad. Sci.* **2009**, *1161*, 1–25. [CrossRef]

145. Khellaf, B.; Boussad, B. Computational Hemodynamic Investigation of a New Bileaflet Mechanical Heart Valve. *Simulation* **2020**, *96*, 459–469. [CrossRef]

146. Hanafizadeh, P.; Mirkhani, N.; Davoudi, M.R.; Masouminia, M.; Sadeghy, K. Non-Newtonian Blood Flow Simulation of Diastolic Phase in Bileaflet Mechanical Heart Valve Implanted in a Realistic Aortic Root Containing Coronary Arteries. *Artif. Organs* **2016**, *40*, E179–E191. [CrossRef]

147. Simon, H.A.; Dasi, L.P.; Leo, H.L.; Yoganathan, A.P. Spatio-Temporal Flow Analysis in Bileaflet Heart Valve Hinge Regions: Potential Analysis for Blood Element Damage. *Ann. Biomed. Eng.* **2007**, *35*, 1333–1346. [CrossRef] [PubMed]

148. Mohammadi, H.; Ahmadian, M.T.; Wan, W.K. Time-Dependent Analysis of Leaflets in Mechanical Aortic Bileaflet Heart Valves in Closing Phase Using the Finite Strip Method. *Med. Eng. Phys.* **2006**, *28*, 122–133. [CrossRef] [PubMed]

149. Amiri Delouei, A.; Nazari, M.; Kayhani, M.H.; Succi, S. Non-Newtonian Unconfined Flow and Heat Transfer over a Heated Cylinder Using the Direct-Forcing Immersed Boundary-Thermal Lattice Boltzmann Method. *Phys. Rev. E Stat. Nonlin Soft Matter. Phys.* **2014**, *89*, 053312. [CrossRef] [PubMed]

150. Afra, B.; Delouei, A.A.; Tarokh, A. Flow-Induced Locomotion of a Flexible Filament in the Wake of a Cylinder in Non-Newtonian Flows. *Int. J. Mech. Sci.* **2022**, *234*, 107693. [CrossRef]

151. Afra, B.; Karimnejad, S.; Amiri Delouei, A.; Tarokh, A. Flow Control of Two Tandem Cylinders by a Highly Flexible Filament: Lattice Spring IB-LBM. *Ocean Eng.* **2022**, *250*, 111025. [CrossRef]

152. Gilmanov, A.; Barker, A.; Stolarski, H.; Sotiropoulos, F. Image-Guided Fluid-Structure Interaction Simulation of Transvalvular Hemodynamics: Quantifying the Effects of Varying Aortic Valve Leaflet Thickness. *Fluids* **2019**, *4*, 119. [CrossRef]

153. Gilmanov, A.; Stolarski, H.; Sotiropoulos, F. Non-Linear Rotation-Free Shell Finite-Element Models for Aortic Heart Valves. *J. Biomech.* **2017**, *50*, 56–62. [CrossRef]

154. Gilmanov, A.; Stolarski, H.; Sotiropoulos, F. Flow-Structure Interaction Simulations of the Aortic Heart Valve at Physiologic Conditions: The Role of Tissue Constitutive Model. *J. Biomech. Eng.* **2018**, *140*, 041003. [CrossRef]

155. Chen, Y.; Luo, H. A Computational Study of the Three-Dimensional Fluid–Structure Interaction of Aortic Valve. *J. Fluids Struct.* **2018**, *80*, 332–349. [CrossRef]

156. Laadhari, A.; Székely, G. Eulerian Finite Element Method for the Numerical Modeling of Fluid Dynamics of Natural and Pathological Aortic Valves. *J. Comput. Appl. Math.* **2017**, *319*, 236–261. [CrossRef]

157. Soltany Sadrabadi, M.; Hedayat, M.; Borazjani, I.; Arzani, A. Fluid-Structure Coupled Biotransport Processes in Aortic Valve Disease. *J. Biomech.* **2021**, *117*, 110239. [CrossRef]

158. Torrado, A. Analysis of Hemodynamic Indicators in Bicuspid Aortic Valves Using a Computational Mathematical Model. Ph.D. Thesis, Instituto Superior Técnico, Lisboa, Portugal, 2015.

159. Luraghi, G.; Migliavacca, F.; García-González, A.; Chiastra, C.; Rossi, A.; Cao, D.; Stefanini, G.; Rodriguez Matas, J.F. On the Modeling of Patient-Specific Transcatheter Aortic Valve Replacement: A Fluid–Structure Interaction Approach. *Cardiovasc. Eng. Technol.* **2019**, *10*, 437–455. [CrossRef] [PubMed]

160. Luraghi, G.; Wu, W.; De Gaetano, F.; Rodriguez Matas, J.F.; Moggridge, G.D.; Serrani, M.; Stasiak, J.; Costantino, M.L.; Migliavacca, F. Evaluation of an Aortic Valve Prosthesis: Fluid-Structure Interaction or Structural Simulation? *J. Biomech.* **2017**, *58*, 45–51. [CrossRef] [PubMed]

161. Johnson, N.P.; Zelis, J.M.; Tonino, P.A.L.; Houthuizen, P.; Bouwman, R.A.; Brueren, G.R.G.; Johnson, D.T.; Koolen, J.J.; Korsten, H.H.M.; Wijnbergen, I.F.; et al. Pressure Gradient vs. Flow Relationships to Characterize the Physiology of a Severely Stenotic Aortic Valve before and after Transcatheter Valve Implantation. *Eur. Heart J.* **2018**, *39*, 2646–2655. [CrossRef] [PubMed]

162. Zelis, J.M.; Tonino, P.A.L.; Johnson, D.T.; Balan, P.; Brueren, G.R.G.; Wijnbergen, I.; Kirkeeide, R.L.; Pijls, N.H.J.; Gould, K.L.; Johnson, N.P. Stress Aortic Valve Index (SAVI) with Dobutamine for Low-Gradient Aortic Stenosis: A Pilot Study. *Struct. Heart* **2020**, *4*, 53–61. [CrossRef]

163. Biffi, B.; Bosi, G.M.; Lintas, V.; Jones, R.; Tzamtzis, S.; Burriesci, G.; Migliavacca, F.; Taylor, A.M.; Schievano, S.; Biglino, G. Numerical Model of a Valvuloplasty Balloon: In Vitro Validation in a Rapid-Prototyped Phantom. *Biomed. Eng. Online* **2016**, *15*, 37. [CrossRef]

164. Luraghi, G.; Migliavacca, F.; Chiastra, C.; Rossi, A.; Reimers, B.; Stefanini, G.G.; Rodriguez Matas, J.F. Does Clinical Data Quality Affect Fluid-Structure Interaction Simulations of Patient-Specific Stenotic Aortic Valve Models? *J. Biomech.* **2019**, *94*, 202–210. [CrossRef]

165. Martin, C.; Sun, W. Transcatheter Valve Underexpansion Limits Leaflet Durability: Implications for Valve-in-Valve Procedures. *Ann. Biomed. Eng.* **2017**, *45*, 394–404. [CrossRef]

166. Dasi, L.P.; Hatoum, H.; Kheradvar, A.; Zareian, R.; Alavi, S.H.; Sun, W.; Martin, C.; Pham, T.; Wang, Q.; Midha, P.A.; et al. On the Mechanics of Transcatheter Aortic Valve Replacement. *Ann. Biomed. Eng.* **2017**, *45*, 310–331. [CrossRef]

167. Pasta, S.; Cannata, S.; Gentile, G.; Di Giuseppe, M.; Cosentino, F.; Pasta, F.; Agnese, V.; Bellavia, D.; Raffa, G.M.; Pilato, M.; et al. Simulation Study of Transcatheter Heart Valve Implantation in Patients with Stenotic Bicuspid Aortic Valve. *Med. Biol. Eng. Comput.* **2020**, *58*, 815–829. [CrossRef] [PubMed]

168. Pasta, S.; Gandolfo, C. Computational Analysis of Self-Expanding and Balloon-Expandable Transcatheter Heart Valves. *Biomechanics* **2021**, *1*, 43–52. [CrossRef]

169. Van Aswegen, K.H.J.; Smuts, A.N.; Scheffer, C.; Weich, H.S.V.; Doubell, A.F. Investigation of Leaflet Geometry in a Percutaneous Aortic Valve with the Use of Fluid-Structure Interaction Simulation. *J. Mech. Med. Biol.* **2012**, *12*, 1250003. [CrossRef]

170. Govindarajan, V.; Kolanjiyil, A.; Johnson, N.P.; Kim, H.; Chandran, K.B.; McPherson, D.D. Improving Transcatheter Aortic Valve Interventional Predictability via Fluid-Structure Interaction Modelling Using Patient-Specific Anatomy. *R Soc. Open Sci.* **2022**, *9*, 211694. [CrossRef] [PubMed]
171. Weinberg, E.J.; Mofrad, M.R.K. Three-Dimensional, Multiscale Simulations of the Human Aortic Valve. *Cardiovasc. Eng.* **2007**, *7*, 140–155. [CrossRef] [PubMed]
172. Conti, C.A.; Votta, E.; Della Corte, A.; Del Viscovo, L.; Bancone, C.; Cotrufo, M.; Redaelli, A. Dynamic Finite Element Analysis of the Aortic Root from MRI-Derived Parameters. *Med. Eng. Phys.* **2010**, *32*, 212–221. [CrossRef]
173. Bianchi, D.; Monaldo, E.; Gizzi, A.; Marino, M.; Filippi, S.; Vairo, G. A FSI Computational Framework for Vascular Physiopathology: A Novel Flow-Tissue Multiscale Strategy. *Med. Eng. Phys.* **2017**, *47*, 25–37. [CrossRef]
174. Pasta, S.; Cannata, S.; Gentile, G.; Agnese, V.; Raffa, G.M.; Pilato, M.; Gandolfo, C. Transcatheter Heart Valve Implantation in Bicuspid Patients with Self-Expanding Device. *Bioengineering* **2021**, *8*, 91. [CrossRef]
175. Colombo, A.; Latib, A. Bicuspid Aortic Valve: Any Room for TAVR? *J. Am. Coll Cardiol.* **2014**, *64*, 2340–2342. [CrossRef]
176. Guyton, R.A.; Padala, M. Transcatheter Aortic Valve Replacement in Bicuspid Aortic Stenosis Early Success but Concerning Red Flags. *JACC Cardiovasc. Interv.* **2016**, *9*, 825–827. [CrossRef]
177. Makkar, R.; Chakravarty, T.; Jilaihawi, H. Transcatheter Aortic Valve Replacement for Bicuspid Aortic Stenosis: Are We Ready for the Challenge? *J. Am. Coll Cardiol.* **2016**, *68*, 1206–1208. [CrossRef]
178. Esmailie, F.; Razavi, A.; Yeats, B.; Sivakumar, S.K.; Chen, H.; Samaee, M.; Shah, I.A.; Veneziani, A.; Yadav, P.; Thourani, V.H.; et al. Biomechanics of Transcatheter Aortic Valve Replacement Complications and Computational Predictive Modeling. *Struct. Heart* **2022**, *6*, 100032. [CrossRef]
179. Dalmau, M.J.; González-Santos, J.M.; Blázquez, J.A.; Sastre, J.A.; López-Rodríguez, J.; Bueno, M.; Castaño, M.; Arribas, A. Hemodynamic Performance of the Medtronic Mosaic and Perimount Magna Aortic Bioprostheses: Five-Year Results of a Prospectively Randomized Study. *Eur. J. Cardio-Thorac. Surg.* **2011**, *39*, 844–852. [CrossRef]
180. Andreas, M.; Wallner, S.; Ruetzler, K.; Wiedemann, D.; Ehrlich, M.; Heinze, G.; Binder, T.; Moritz, A.; Hiesmayr, M.J.; Kocher, A.; et al. Comparable Long-Term Results for Porcine and Pericardial Prostheses after Isolated Aortic Valve Replacement. *Eur. J. Cardio-Thorac. Surg.* **2015**, *48*, 557–561. [CrossRef]
181. Wagner, I.M.; Eichinger, W.B.; Bleiziffer, S.; Botzenhardt, F.; Gebauer, I.; Guenzinger, R.; Bauernschmitt, R.; Lange, R. Influence of Completely Supra-Annular Placement of Bioprostheses on Exercise Hemodynamics in Patients with a Small Aortic Annulus. *J. Thorac. Cardiovasc. Surg.* **2007**, *133*, 1234–1241. [CrossRef]
182. Yap, K.H.; Murphy, R.; Devbhandari, M.; Venkateswaran, R. Aortic Valve Replacement: Is Porcine or Bovine Valve Better? *Interact. Cardiovasc. Thorac. Surg.* **2013**, *16*, 361–373. [CrossRef]
183. Borger, M.A.; Nette, A.F.; Maganti, M.; Feindel, C.M. Carpentier-Edwards Perimount Magna Valve Versus Medtronic Hancock II: A Matched Hemodynamic Comparison. *Ann. Thorac. Surg.* **2007**, *83*, 2054–2058. [CrossRef]
184. Marn, J.; Iljaž, J.; Žunič, Z.; Ternik, P. Non-Newtonian Blood Flow around Healthy and Regurgitated Aortic Valve with Coronary Blood Flow Involved. *Stroj. Vestn. J. Mech. Eng.* **2012**, *58*, 482–491. [CrossRef]
185. Wong, I.; Sondergaard, L.; De Backer, O. Computational Simulation Models to Test Bioprosthetic Aortic Valves: A Valuable Alternative or Addition to Bench Testing? *Int. J. Cardiol.* **2021**, *340*, 66–67. [CrossRef]
186. Chan, V.; Kulik, A.; Tran, A.; Hendry, P.; Masters, R.; Mesana, T.G.; Ruel, M. Long-Term Clinical and Hemodynamic Performance of the Hancock II versus the Perimount Aortic Bioprostheses. *Circulation* **2010**, *122*, S10–S16. [CrossRef]
187. Hickey, G.L.; Grant, S.W.; Bridgewater, B.; Kendall, S.; Bryan, A.J.; Kuo, J.; Dunning, J. A Comparison of Outcomes between Bovine Pericardial and Porcine Valves in 38 040 Patients in England and Wales over 10 Years. *Eur. J. Cardio-Thorac. Surg.* **2014**, *47*, 1067–1074. [CrossRef]
188. Einstein, D.R.; Kunzelman, K.S.; Reinhall, P.G.; Nicosia, M.A.; Cochran, R.P. Non-Linear Fluid-Coupled Computational Model of the Mitral Valve. *J. Heart Valve Dis.* **2005**, *14*, 376–385. [PubMed]
189. Huang, H.S. Micromechanical Simulations of Heart Valve Tissues. Ph.D. Thesis, University of Pittsburgh, Pittsburgh, PA, USA, 2004.
190. Khang, A.; Buchanan, R.M.; Ayoub, S.; Rego, B.V.; Lee, C.H.; Ferrari, G.; Anseth, K.S.; Sacks, M.S. Mechanobiology of the Heart Valve Interstitial Cell: Simulation, Experiment, and Discovery. In *Mechanobiology in Health and Disease*; Academic Press: Cambridge, MA, USA, 2018; pp. 249–283. ISBN 9780128129524. [CrossRef]
191. Nowak, M.; Divo, E.; Adamczyk, W.P. Multiscale Model for Blood Flow after a Bileaflet Artificial Aortic Valve Implantation. *Comput. Biol. Med.* **2023**, *158*, 106805. [CrossRef]
192. Borazjani, I.; Sotiropoulos, F. The Effect of Implantation Orientation of a Bileaflet Mechanical Heart Valve on Kinematics and Hemodynamics in an Anatomic Aorta. *J. Biomech. Eng.* **2010**, *132*, 111005. [CrossRef]
193. Allen, P.; Robertson, R. The Significance of Intermittent Regurgitation in Aortic Valve Prostheses. *J. Thorac. Cardiovasc. Surg.* **1967**, *54*, 549–552. [CrossRef]
194. Khalili, F.; Gamage, P.P.T.; Sandler, R.H.; Mansy, H.A. Adverse Hemodynamic Conditions Associated with Mechanical Heart Valve Leaflet Immobility. *Bioengineering* **2018**, *5*, 74. [CrossRef]
195. Le, T.B.; Usta, M.; Aidun, C.; Yoganathan, A.; Sotiropoulos, F. Computational Methods for Fluid-Structure Interaction Simulation of Heart Valves in Patient-Specific Left Heart Anatomies. *Fluids* **2022**, *7*, 94. [CrossRef]

196. Mourato, A.; Valente, R.; Xavier, J.; Brito, M.; Avril, S.; de Sá, J.C.; Tomás, A.; Fragata, J. Computational Modelling and Simulation of Fluid Structure Interaction in Aortic Aneurysms: A Systematic Review and Discussion of the Clinical Potential. *Appl. Sci.* **2022**, *12*, 8049. [CrossRef]

197. Kuchumov, A.G.; Nyashin, Y.I.; Samartsev, V.A.; Tuktamyshev, V.S.; Lokhov, V.A.; Shestakov, A.P. Mathematical Modelling of Shape Memory Stent Placing at Endobiliary Interventions. *Russ. J. Biomech.* **2017**, *21*, 394–404.

198. Sinelnikov, Y.S.; Arutunyan, V.B.; Porodikov, A.A.; Biyanov, A.N.; Tuktamyshev, V.S.; Shmurak, M.I.; Khairulin, A.R.; Kuchumov, A.G. Application of Mathematical Modelling for the Evaluation of the Results of Systemic-Pulmonary Shunts Formation. *Patol. Krovoobrashcheniya I Kardiokhirurgiya* **2020**, *24*, 45–61. [CrossRef]

199. Kuchumov, A.G.; Kamaltdinov, M.R.; Samartsev, V.A.; Khairulin, A.R.; Ivashova, Y.A.; Taiar, R. Patient-Specific Simulation of a Gallbladder Refilling Based on MRI and Ultrasound in Vivo Measurements. *AIP Conf. Proc.* **2020**, *2216*, 060004.

200. Kuchumov, A.G.; Khairulin, A.R.; Biyanov, A.N.; Porodikov, A.A.; Arutyunyan, V.B.; Sinelnikov, Y.S. Effectiveness of Blalock-Taussig Shunt Performance in the Congenital Heart Disease Children. *Russ. J. Biomech.* **2020**, *24*, 65–83.

201. Bailoor, S.; Seo, J.H.; Dasi, L.P.; Schena, S.; Mittal, R. A Computational Study of the Hemodynamics of Bioprosthetic Aortic Valves with Reduced Leaflet Motion. *J. Biomech.* **2021**, *120*, 110350. [CrossRef] [PubMed]

202. Lone, T.; Alday, A.; Zakerzadeh, R. Numerical Analysis of Stenoses Severity and Aortic Wall Mechanics in Patients with Supravalvular Aortic Stenosis. *Comput. Biol. Med.* **2021**, *135*, 104573. [CrossRef] [PubMed]

203. Sigüenza, J.; Pott, D.; Mendez, S.; Sonntag, S.J.; Kaufmann, T.A.S.; Steinseifer, U.; Nicoud, F. Fluid-Structure Interaction of a Pulsatile Flow with an Aortic Valve Model: A Combined Experimental and Numerical Study. *Int. J. Numer. Method Biomed. Eng.* **2018**, *34*, e2945. [CrossRef]

204. Bavo, A.M.; Rocatello, G.; Iannaccone, F.; Degroote, J.; Vierendeels, J.; Segers, P. Fluid-Structure Interaction Simulation of Prosthetic Aortic Valves: Comparison between Immersed Boundary and Arbitrary Lagrangian-Eulerian Techniques for the Mesh Representation. *PLoS ONE* **2016**, *11*, e0154517. [CrossRef] [PubMed]

205. Carmody, C.J.; Burriesci, G.; Howard, I.C.; Patterson, E.A. An Approach to the Simulation of Fluid-Structure Interaction in the Aortic Valve. *J. Biomech.* **2006**, *39*, 158–169. [CrossRef]

206. Bucelli, M.; Zingaro, A.; Africa, P.C.; Fumagalli, I.; Dede', L.; Quarteroni, A. A Mathematical Model That Integrates Cardiac Electrophysiology, Mechanics, and Fluid Dynamics: Application to the Human Left Heart. *Int. J. Numer. Method Biomed. Eng.* **2023**, *39*, e3678. [CrossRef] [PubMed]

207. Engel, M.; Griebel, M. Flow Simulation on Moving Boundary-Fitted Grids and Application to Fluid-Structure Interaction Problems. *Int. J. Numer. Methods Fluids* **2006**, *50*, 437–468. [CrossRef]

208. Tango, A.M.; Salmonsmith, J.; Ducci, A.; Burriesci, G. Validation and Extension of a Fluid–Structure Interaction Model of the Healthy Aortic Valve. *Cardiovasc. Eng. Technol.* **2018**, *9*, 739–751. [CrossRef]